Thermal Hydraulic (CVH and FL) Packages Reference Manual

Two packages in the MELCOR code, the Control Volume Hydrodynamics (CVH) package and the Flow Path (FL) package, are responsible for modeling the thermal-hydraulic behavior of coolant liquids and gases. The former is concerned with control volumes and their contents, the latter with the connections which allow transfer of these contents between control volumes. The distinction between CVH and FL is useful primarily for discussion of MELCOR input and output. It will frequently be ignored in this Reference Manual, where many aspects of the thermal-hydraulic modeling will be described without concern for which package contains the relevant coding.

If phenomena modeled by other packages in MELCOR influence thermal-hydraulic behavior, the consequences are represented as sources and sinks of mass, energy, or available volume, or as changes in the area or flow resistance of flow paths in CVH. [Changes involving flow paths may currently be handled only through use of the Control Function (CF) package.]

Equations of state for the hydrodynamic materials are contained in the Control Volume Thermodynamics (CVT) package, which in turn makes use of the water properties (H2O) and NonCondensible Gas (NCG) packages.

This Reference Manual describes the assumptions, models, and solution strategies used in the various subroutines which make up the CVH and FL packages. The user is referred to the appropriate Reference Manuals and other documentation for details of the equations of state and the boundary conditions provided by other packages in MELCOR.

Contents

List of Tables

List of Figures

1. Introduction

Thermal-hydraulic processes interact with and are coupled to all aspects of accident phenomenology. In the MELCOR code, thermal-hydraulic data calculated by the Control Volume Hydrodynamics (CVH) and Flow Path (FL) packages provide boundary conditions to other phenomenological packages such as Burn (BUR), Cavity (CAV), Core (COR), Fuel Dispersal Interactions (FDI), and Heat Structures (HS). These packages, in turn, calculate sources and sinks of mass and energy for CVH. COR and HS also calculate changes to the volumes available to hydrodynamic materials. In some cases, CVH results are used directly by another package: the RadioNuclide (RN) package uses CVH results for advection to transport aerosols and vapors from one calculational volume to another; RN also uses CVH results for the liquid water content of the atmosphere (fog) as the water content of aerosols, rather than integrating a separate equation for condensation and evaporation. Therefore, even though the primary interest in accident research is *not* solely thermal-hydraulics, the thermal-hydraulic modeling in CVH and FL forms the backbone of the MELCOR code.

The choice of modeling in CVH and FL was influenced by a number of often conflicting requirements. The packages were desired to be computationally fast, but also reliable and accurate. They should not produce minor nonphysical variations in behavior that would adversely affect the performance of other packages, and should not be unduly sensitive to such variations in the conditions calculated by other packages. They should permit great flexibility in nodalization to simplify sensitivity studies and should extract the maximum amount of information from coarse nodalizations while allowing more detailed ones for comparison to more specialized codes. In addition, they should be user friendly with respect to input.

The calculational method chosen uses a control volume/flow path approach similar to RELAP4 [1], HECTR [2], and CONTAIN [3]. The same models and solution algorithms are used for all volumes; i.e., the primary, secondary, and containment volumes are modeled consistently and the resulting equations are solved simultaneously. Within the basic control volume formulation, the treatment is quite general; unlike the MAAP code [4], no specific nodalization is built in. No component models are explicitly included; pipes, vessels, pressurizers, steam generators, etc., are built through user input from control volumes, flow paths, and elements of other packages such as heat structures. Control logic used to simulate active or passive systems is introduced using control functions. (There are separate models for a few special safety systems including fan coolers and containment sprays.) We anticipate that, as experience with MELCOR grows, a set of "standard" nodalizations will be developed, validated, and employed for most calculations. However the freedom exists to investigate sensitivities to variations in nodalization (and to develop representations of systems) entirely from code input, without modification to MELCOR itself.

A semi-implicit (linearized) formulation of the governing equations is used to permit timesteps greater than the acoustic Courant limit. The numerical solution technique is similar to that in RELAP4 [1], with two major differences: (1) MELCOR uses a full two-fluid treatment rather than the drift-flux formulation of RELAP4 and (2) the resulting equations are iterated when necessary so that the result is fully implicit with respect to pressures used in the momentum equation. A significant feature of this method is that the resulting equations are exactly conservative (to within machine roundoff) with respect to masses and to thermal energy.

All hydrodynamic material in a MELCOR calculation, together with its energy, resides in *control volumes*. "Hydrodynamic material" includes the coolant (water), vapor (steam), and noncondensible gases; it does not include the core or core debris, other structures, fission products, aerosols, or water films on heat structures. The hydrodynamic materials are divided into two independent fields referred to as *pool* and *atmosphere*. The names refer to the frequently-employed picture of separation under gravity within a control volume, but the actual interpretation is less restrictive. The shape of the volume is defined in enough detail to allow the elevation of the pool surface to be determined. Beyond this, a control volume has no internal structure and is characterized by a single pressure and two temperatures, one temperature for the pool and one for the atmosphere. (Of course, various constitutive models in CVH/FL and other packages may *infer* greater detail such as boundary and interface temperatures, and temperature or pressure gradients, but they are not part of the CVH/FL database.)

The control volumes are connected by *flow paths* through which the hydrodynamic materials may move without residence time, driven by a separate momentum equation for each field. Each control volume may be connected to an arbitrary number of others and parallel flow paths (connecting the same pair of volumes) are permitted. There are no restrictions on the connectivity of the network built up in this way. Both pool and atmosphere, pool only, or atmosphere only may pass through each flow path, based on the elevations of the pool surfaces in the connected control volumes relative to the junctions with the flow paths. Appropriate hydrostatic head terms are included in the momentum equations for the flow paths, allowing calculation of natural circulation.

The control volumes and flow paths may be used to model physical systems in a variety of ways. In some cases, the control volumes may correspond to physical tanks, with the flow paths representing pipes (of negligible volume) connecting them. In others, the volumes may be geometrical regions—perhaps portions of larger physical rooms—with the flow paths representing the geometrical surfaces separating them. Representations approaching a finite difference approximation to the one-, two-, or three-dimensional hydrodynamic equations may be built up using the latter approach. However, because the momentum equation for each flow path is only one-dimensional and there is no momentum associated with a control volume, multidimensional effects associated with advection of momentum ("momentum flux") cannot be correctly calculated. (The one-dimensional momentum flux term for the direction of flow may be optionally included.)

In addition to phenomena within the CVH and FL packages, calculations performed in other packages in MELCOR may lead to sources and sinks of mass or energy in control volumes, or to changes in the volume available to hydrodynamic materials. These are imposed as numerically explicit boundary conditions in CVH/FL. In addition to heat sources from the Decay Heat (DCH) package, mass and energy source/sinks include heat from the HS, COR, CAV, and FDI packages, water from condensation or evaporation of films or melting of ice in the HS package or deposition of aerosol droplets in the RN package, and various gas sources from outgassing of structures in the HS package or from concrete ablation in the CAV package.

Oxidation chemistry in the COR and BUR packages is modeled as a sink of reactants (water vapor or oxygen in COR, hydrogen or carbon monoxide in BUR) and a source of reaction products (hydrogen in COR, water vapor or carbon dioxide in BUR). All equations of state referenced by the Control Volume Thermodynamics (CVT) package employ consistent thermochemical reference points, with the heat of formation included in the enthalpy functions as in JANAF tables [5]. Therefore, no energy source is involved in such a reaction; total energy is conserved, and the “heat of reaction” associated with changes in chemical bonding energies appears as sensible heat because of changes in the reference-point enthalpy of the system.

Changes in available volume result from such phenomena as candling (relocation of molten core materials by downward flow along fuel rods) and core collapse, which move nonhydrodynamic materials into or out of a control volume. Nonhydrodynamic materials may be moved by other packages either independently of CVH/FL flows (e.g., core relocation) or piggybacked on the flows (e.g., motion of aerosols and associated radionuclides).

2. Basic Control Volume Concepts

The basic concepts, definitions, and terminology associated with control volumes are described in this section. Most of the details of the models will be deferred until after the conservation equations have been presented and discussed.

2.1 Control Volume Geometry

The spatial geometry within a control volume is defined by a *volume/altitude* table. (The terms “altitude” and “elevation” will be used interchangeably in this manual.) Each point in the table gives an altitude and the total volume available to hydrodynamic materials in the CVH package below that altitude in that control volume. In this usage, “altitude” means elevation with respect to some reference point. This reference point is arbitrary, but must be consistent throughout all input for any problem (i.e., the same for all CVH, FL, COR, HS, and other data) to allow differences in elevation to be evaluated correctly.

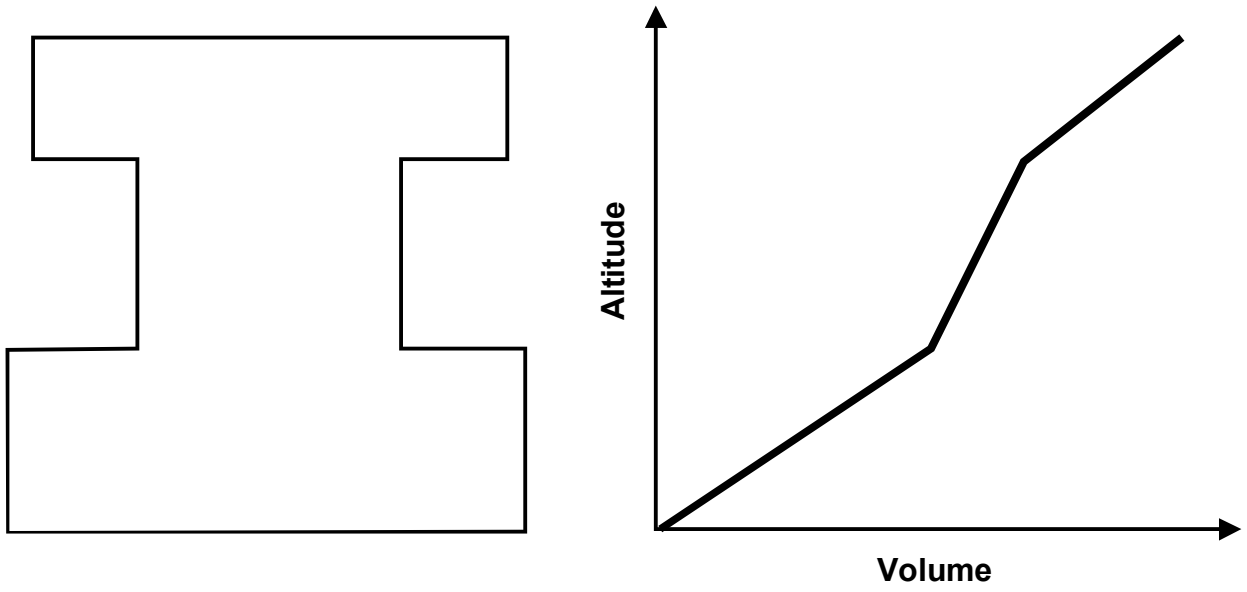

Figure 2.1 Relation of Spatial Volume to Volume/Altitude Table

The volume at the lowest altitude must be zero; the volume is assumed to be a linear function of altitude between table entries. This is equivalent to assuming a piecewise-constant cross-sectional area as illustrated in Figure 2.1, which shows a simple geometric volume and a plot of the corresponding 4-point volume/altitude table. Note that the independent variable, altitude, is plotted vertically to facilitate comparison with the sketch.

In addition to the hydrodynamic volume, a control volume may also contain *virtual volume* associated with nonhydrodynamic material (in some other package) that occupies space but is subject to relocation. If this material is relocated, the space which it occupied will become available to hydrodynamic materials. The principal example of this is the core, which initially occupies a large volume in the primary system, but may melt down and relocate to another part of the primary or containment system. This frees some or all of the original space to be occupied by hydrodynamic materials, while denying space to such materials in the new location.

The initial hydrodynamic volume is defined by input of CVnnnBk records to CVH in MELGEN, and the initial virtual volume is defined by input to other packages. Their sum is calculated in MELGEN for the set of altitude points in the CVH input to define a total volume/altitude table which becomes part of the CVH database and does not change with time. The virtual volume is also carried in the CVH database as a volume/altitude table defined for the set of altitudes input to CVH. The difference between total and virtual volume is available to hydrodynamic materials, and initially coincides with that specified in CVH input.

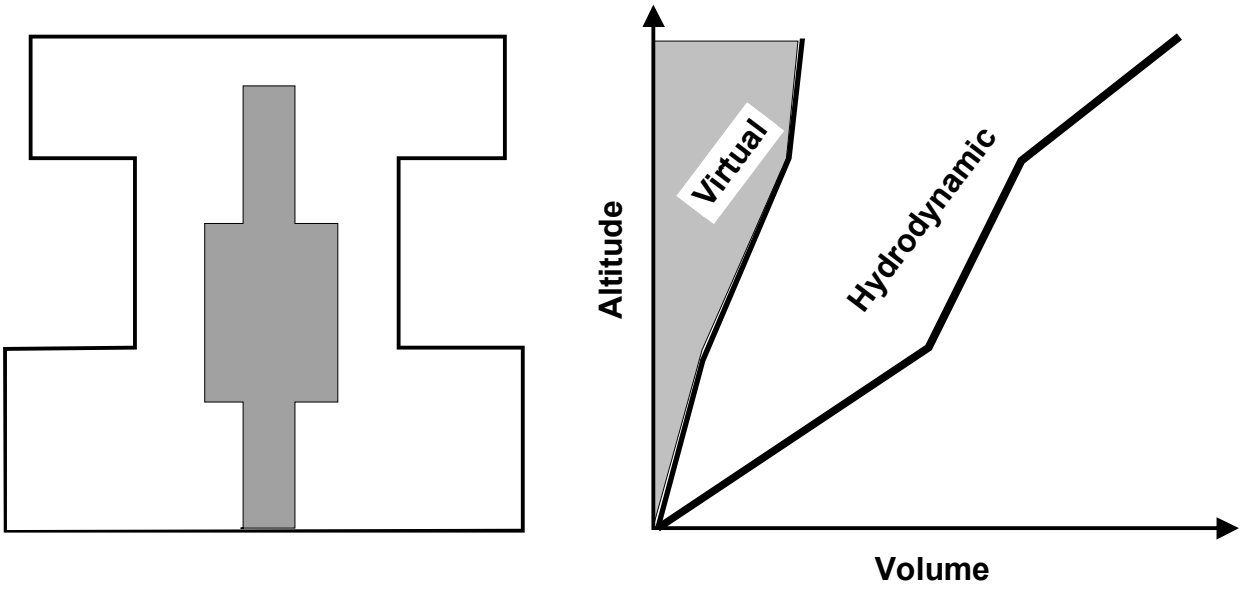

Figure 2.2 Virtual Volume and Associated Volume/Altitude Tables

Virtual volume is illustrated by Figure 2.2, where the total volume is shown in grey and the virtual volume as the white space (i.e., volume on the RHS graph) between the virtual volume and the cell boundary. Note that the points in the virtual-volume/altitude table correspond to the altitudes in the CVH database and not to those in whatever package defined the occupied (shaded) region.

Virtual volume within a control volume is modified as nonhydrodynamic materials are relocated by their controlling packages. In consequence, the hydrodynamic volume is also modified as the space which was occupied by nonhydrodynamic materials becomes available and the space it now occupies is denied to the hydrodynamic materials. The other packages may track the location of their materials in more (or less) detail than is permitted by the set of altitudes recognized by CVH; this has no effect on hydrodynamic calculations.

2.2 Control Volume Contents

The contents of each volume are divided into a so-called *pool* and an *atmosphere*. These terms reflect a static, gravitationally separated situation, such as would exist in containment or in a primary system in the absence of strong forced circulation by pumps, and we conventionally depict the pool as occupying the lower portion of the control volume while the atmosphere fills the remainder. However, as discussed later, this picture is not interpreted so narrowly that it invalidates the use of MELCOR hydrodynamics in other situations.

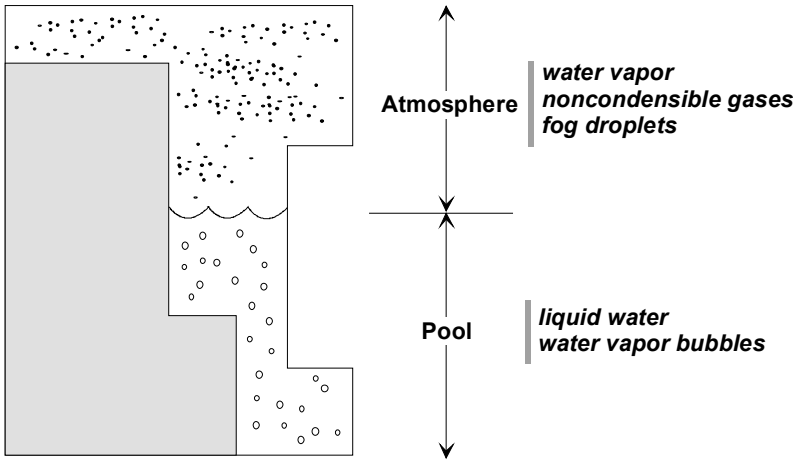

Figure 2.3 Control Volume Contents and Pool Surface

The pool can be single phase liquid water or, in nonequilibrium volumes as discussed below, two-phase (bubbly) water. No noncondensible gases are resident in the pool, although they may flow through and interact with it during a timestep. The atmosphere contains water vapor and/or noncondensible gases, and may also include suspended water droplets, referred to as *fog*. The total volume is divided among pool, gaseous atmosphere, and fog, as shown in Figure 2.3. When needed by submodels, the pool surface is assumed to be a horizontal plane. Its elevation is defined from the volume of the pool by interpolation in the volume/altitude table for the control volume. Only the average void fraction in the pool is part of the CVH database, although a variation of void fraction with elevation may be assumed in submodels.

Materials are numbered in MELCOR. Materials 1, 2, and 3 are always pool, fog, and atmospheric water vapor, respectively. In particular, material 1 includes all of the pool, both liquid water and vapor bubbles. Materials with numbers greater than 3 are noncondensible gases. They are present in a calculation only if specified by the user, in which case their identities depend on input to the NCG package.

2.3 Control Volume Thermodynamic Properties

Given the volume and the mass and energy contents of a control volume, all of its thermodynamic properties are defined by an equation of state. There are two basic options available, selected by user input on record CVnnn00: equilibrium and nonequilibrium.

In MELCOR, equilibrium thermodynamics assumes that the pool and the atmosphere are in thermal and mechanical equilibrium, i.e., that they have the same temperature and pressure. The two subvolumes, pool and atmosphere, are also assumed to be in equilibrium with respect to condensation/evaporation of water.

Nonequilibrium thermodynamics, on the other hand, assumes that while each subvolume is in internal equilibrium, it is in only mechanical equilibrium with the other. That is, neither thermal nor phase equilibrium is assumed between the pool and the atmosphere. (Note that this is *not* nonequilibrium in the sense of TRAC [6] or RELAP5 [7].) While the pressures of the pool and the atmosphere are equal, their temperatures may be different, and there may be a substantial driving force for condensation or evaporation. The distinction between equilibrium and nonequilibrium thermodynamics exists only if a control volume contains both a pool and an atmosphere. The calculations required to determine the necessary thermodynamic properties (pressure, temperature, etc.) in either case are performed in the Control Volume Thermodynamics (CVT) package; for a detailed description, see the CVT Reference Manual.

For equilibrium thermodynamics, only the total energy content of a control volume is relevant, because CVT will reapportion the total energy so as to obtain equilibrium among species in the atmosphere and between the atmosphere and the pool. This implies effectively instantaneous mass and energy transfer between pool and atmosphere, and the explicit calculation of the exchange terms is eliminated in favor of simple assumptions. All water vapor is currently assumed to be in the atmosphere. Liquid water, however, can exist both in the pool and as fog in the atmosphere. An auxiliary calculation is used to determine the partition. For more details, see Section 2.4 of the CVT Reference Manual.

The exchange terms must be calculated, however, for volumes in which nonequilibrium thermodynamics is prescribed. An additional term, the PdV work done by the pool on the atmosphere (or vice versa) as a result of motion of the pool surface, must also be kept in mind in the nonequilibrium case; it is actually accounted for (as $P \Delta V$) in CVT.

When nonhydrodynamic materials are relocated, changing the volume available to hydrodynamic materials, work is done in the process. This work is currently ignored in the package responsible for the relocation; that is, the energy inventory of that package is not affected. The error involved is insignificant in most cases because nonhydrodynamic materials are not ordinarily relocated through large pressure differentials and the net work done is therefore very small. Pressure differentials can be large during high pressure melt ejection in the Fuel Dispersal Interactions (FDI) package, but even there the work term is small compared to other energy exchanges. However, the work must be included in CVH; for purposes of global energy accounting, it is treated as being created there.

The single pressure that CVH assigns to a control volume is assumed to correspond to the elevation of the pool/atmosphere interface. If there is no pool, this is taken as the bottom of the control volume; if there is no atmosphere, it is taken as the top. This choice (as opposed to a volume-centered pressure) simplifies the treatment of condensation/ evaporation rates at the interface. As discussed below, the hydrostatic head corresponding to the difference between the pool-surface reference elevation and the junction of a flow path to a control volume is accounted for in the momentum equation—such a head term would be necessary for *any* definition of the reference elevation for the pressure in a control volume.

3. Basic Flow Path Concepts

The basic concepts, definitions, and models associated with flow paths are described in this section. Most of the details will be deferred until after the conservation equations have been presented and their solution discussed.

3.1 Flow Path Definition

Each flow path connects two control volumes, specified on input record FLnnn00. One is referred to as the *from* volume and the other as the *to* volume, thus defining the direction of positive flow. An arbitrary number of flow paths may be connected to or from each control volume; parallel paths (connecting the same two volumes) are allowed.

Mass and energy are advected through the flow paths, from one volume to another, in response to solutions of the momentum (flow) equation. No volume, mass, or energy is associated with a flow path itself, and no heat structures are allowed to communicate directly with the material passing through it. Therefore, the effect of advection through a flow path is to remove mass and energy from one control volume and to deposit it directly into another control volume. The formulation is manifestly conservative with respect to both mass and energy, because there is a detailed balance between gains and losses in the two volumes connected by each flow path.

The cross-sectional area of a flow path is shared by pool and atmosphere in accordance with a calculated void fraction based on geometry and flow directions. The velocities of pool and atmosphere may be different if both are permitted to flow by the void fraction model; the directions of flow may even be opposite, i.e., countercurrent.

3.2 Flow Path Geometry

Flow path geometry is described on input records FLnnn00 and FLnnn01. Each flow path is characterized by a nominal area and a length. The area may be further modified by a user-controlled *open fraction*, which models (among other things) the effects of valves. The area is used in the conversion of volumetric flows to linear velocities, and is therefore involved in form-loss and critical flow modeling. The length is used in the momentum equation to define the inertia of the flow; as in other codes of this type, the ratio of length to area is the relevant parameter. It should be noted that (unlike some other codes) this inertial length is *not* used in the calculation of frictional pressure drops resulting from wall friction; *segment* data are used instead. Each flow path may be described in terms of a number of segments with differing lengths, areas, hydraulic diameters, surface roughnesses, etc. The details will be discussed in Section 5.4; for now, it is sufficient to note that in the calculation segment data are combined with the flow path form-loss coefficient (optionally defined on input record FLnnn03 for both forward and reverse flow) to form a single effective loss coefficient applied to the flow-path velocity.

Each connection of a flow path to a control volume is referred to as a *junction*, and is characterized by a nominal elevation and an opening height. The opening height defines a range of elevations about the junction elevation over which the flow path sees the contents of the control volume. These two quantities, in conjunction with the elevation of the pool surface, therefore determine whether pool, atmosphere, or both are available for outflow. The junction elevations and heights are also used in the calculation of hydrostatic head terms; the lengths of the flow paths are not.

A flow path may be defined through user input on record FLnnn02 to be *horizontal* or *vertical*. In a control volume/flow path formulation, the orientation of a flow path can not be rigorously defined; the specification affects the definition of junction geometry, below, and the (default) definition of the length over which interphase forces act, described in Section 5.5.

The definition of a junction opening is illustrated in Figure 3.1, which also illustrates the possible truncation of the opening to match the associated control volume.

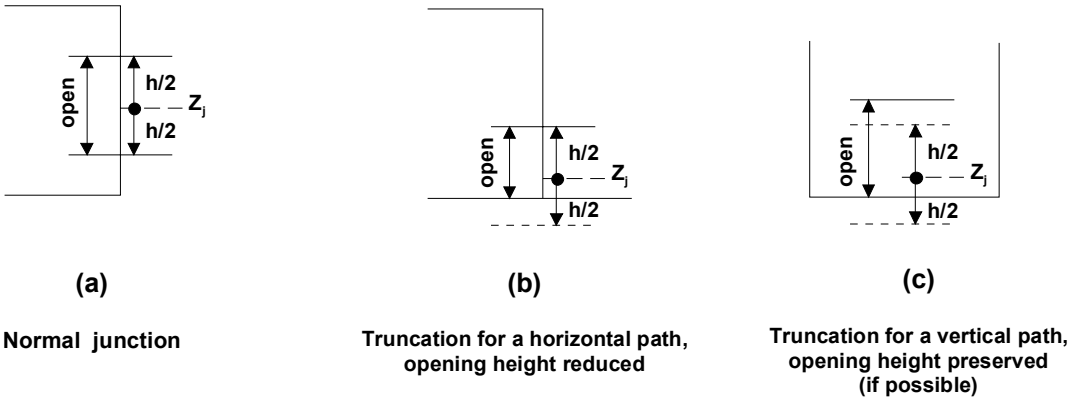

Figure 3.1 Junction Geometry

Each junction elevation is required to lie within the range of elevations associated with the control volume with which it connects; that is, the junction elevation Z_J is required to lie between the bottom, Z_B, and the top, Z_T, of the control volume (inclusive). The junction height, h, is normally considered to be centered on the junction elevation, one half below and the remainder above, and, if the resulting junction opening (between $Z_J - h/2$ and $Z_J + h/2$) extends beyond the limits of the volume, it is truncated. (The nominal junction elevation, Z_J, is not modified.) In the case of a flow path specified by input as vertical (and in this case only), an attempt is made to preserve the full junction height. If the bottom of the junction opening is truncated, its top will be raised a corresponding amount above $Z_J + h/2$ (but not above Z_T). A similar modification is applied if the top of the opening extends above the top of the volume. Input directives allow direct specification of the direct input of the elevations of the top and bottom of junction openings. In this case, no adjustments will be made, and the input will be rejected if the opening extends beyond the limits of the associated volume. As currently implemented, the default definition of junction opening

heights and the treatment of the interphase force are the only differences in treatment between horizontal and vertical flow paths. (Details of the interphase force model are presented in Section 5.5.)

The junction void fraction is determined from the relative positions of the junction opening and the pool surface, and is taken as the fraction of the opening height occupied by atmosphere (in effect, the opening is treated as rectangular). This is illustrated in Figure 3.2. (*Atmosphere fraction* would be a more precise term than *void fraction* because fog flows with the gaseous component of the atmosphere and bubbles flow with the pool.)

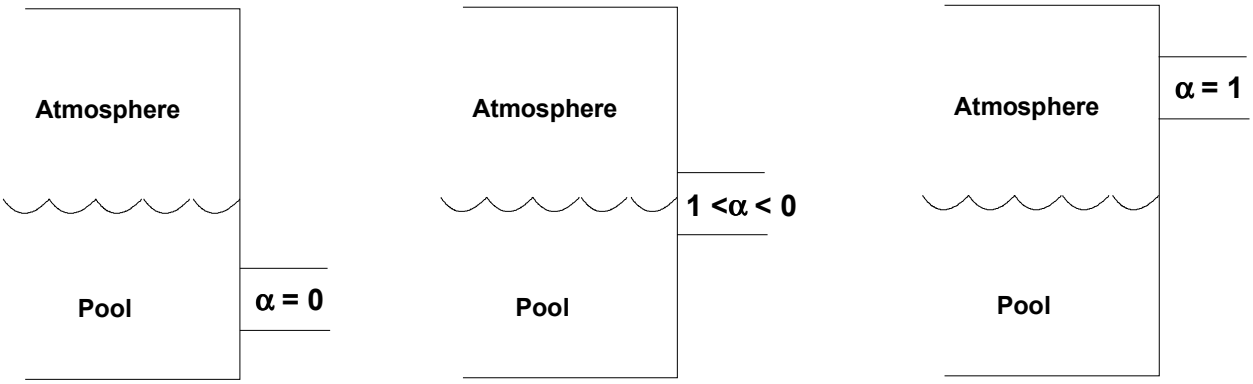

Figure 3.2 Relationship among Junction Opening, Pool Surface Elevation, and Void Fraction

In the tank-and-pipe limit of hydrodynamic modeling, the length, junction elevation and height have relatively clear physical interpretations. It is recommended that the junction height for connection of a *vertical* pipe to a tank should be taken as something like the pipe radius; this models to some extent the two-dimensional distortion of the pool surface when there is flow-through such a connection, as well as eliminating the discontinuity in behavior which would otherwise occur when the pool surface crosses through the junction elevation. Because of this role in eliminating discontinuous behavior, the junction height may not be input as zero.

In the finite-difference limit, a “flow path” represents a surface which is a common boundary between the volumes connected; the length should be taken as roughly the center-to-center distance between volumes, and the elevations of both ends of the junction should be taken as the midpoint elevation of the common boundary. For horizontal flow through a vertical boundary, the junction height should be specified as large enough to include the entire boundary. For vertical flow through a horizontal boundary, the height has no rigorous interpretation; it serves only to define the range of elevations from which material may be drawn.

The flow equations include a term for the interphase force acting between the pool flow and the atmosphere flow in a single flow path. Among other things, this force tends to limit the relative velocity between the phases and can cause entrainment through a vertical flow

path whenever both phases (pool and atmosphere) are present within the junction opening and the interphase force is large enough to overcome the head difference for them. In particular, a flow of atmosphere from a lower volume to a higher one can entrain an upward pool flow (and a downward pool flow can entrain a corresponding downward atmosphere flow), despite an opposing difference in pressure plus head, if the associated junction opening is sufficiently large that both pool and atmosphere are present within the opening height. This tends to "smear" the pool surface slightly for the purposes of flow calculations, and reduces the computational effort in cases where a rising (or falling) pool surface passes through the top (or bottom) of a control volume. We have found that use of an opening height which is a substantial fraction of the volume height frequently works well.

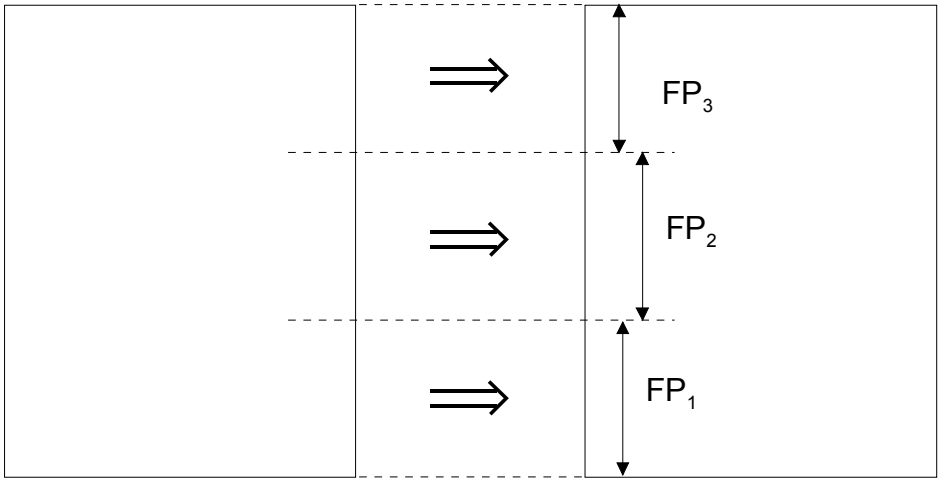

Figure 3.3 Multiple Flow Paths Connecting Two Volumes, to Model Natural Circulation

If is also possible to modify the finite difference limit by dividing the common boundary between two control volumes into two or more parallel flow paths with different elevations, whose areas sum to the correct geometrical total, as illustrated in Figure 3.3. There is preliminary evidence that some aspects of natural convection may be calculable this way.

4. Governing Equations

The governing equations for thermal-hydraulic behavior in MELCOR are the equations of conservation of mass, momentum, and energy. These equations will be presented first as ordinary differential equations for the control-volume formulation, and then in the linearized-implicit finite difference form which is actually solved. They could, of course, be derived by suitable integration of the three-dimensional partial differential equations over a volume (for the scalar mass and energy equations) or along a line (for the vector momentum equation), but the insights to be gained do not justify including the derivation in this Reference Manual. See, for example, Reference [1].

4.1 Ordinary Differential Equations

The differential equation expressing conservation of mass for each material is

$$\frac{\partial \rho}{\partial t} + \nabla \cdot (\rho v) = \Gamma \tag{4.1}$$

where Γ is the volumetric mass source density. Integrated over a control volume, the conservation of mass for material m in control volume i is then expressed by

$$\frac{\partial M_{i,m}}{\partial t} = \sum_j \sigma_{ij} \alpha_{j,\varphi} \rho^d_{j,m} v_{j,\varphi} F_j A_j + \dot{M}_{i,m} \tag{4.2}$$

Here, M is total mass; subscript j refers to flow path, with σ_{ij} accounting for the direction of flow in flow path j with respect to volume i as described below; subscript φ refers to the phase, pool or atmosphere (later abbreviated as "*P*" and "*A*", respectively), in which material m resides; $\alpha_{j,\varphi}$ is the volume fraction of φ in flow path j ($\alpha_{j,A} + \alpha_{j,P} = 1$, see Section 5.2 for definitions); ρ is density; superscript "*d*" denotes "donor", corresponding to the control volume from which material is flowing; v is flow velocity; A is flow path area; F is the fraction of this area which is open; and M includes all non-flow sources, such as condensation/evaporation, bubble separation, fog precipitation, and user-defined sources in CVH, and contributions from other packages in MELCOR.

The summation in Equation (4.2) is over all flow paths, with

$$\sigma_{ij} = \begin{cases} +1 \text{ if path } j \text{ is connected "to" volume } i \\ -1 \text{ if path } j \text{ is connected "from" volume } i \\ 0 \text{ if path } j \text{ is not connected to volume } i \end{cases} \tag{4.3}$$

accounting for which flow paths are actually connected to volume i, and for the direction of positive flow in these paths. As used here, the density is defined by

$$\rho_m \equiv \frac{M_m}{V_\varphi} \tag{4.4}$$

where V_φ is the volume of the phase containing material m. Recall that the pool phase contains single- or two-phase water, while the atmosphere can contain water vapor, noncondensible gases, and liquid water fog.

The equations expressing conservation of energy in the pool and in the atmosphere are derived similarly from the partial differential equations, neglecting all gravitational potential energy and volume-average kinetic energy terms. Conservation of energy in phase φ (pool or atmosphere) is then expressed by

$$\frac{\partial E_{i,\varphi}}{\partial t} = \sum_j \sigma_{ij}\alpha_{j,\varphi}\left(\sum_m \rho^d_{j,m}h^d_{j,m}\right)v_{j,\varphi}F_jA_j + \dot{H}_{i,\varphi} \tag{4.5}$$

where E is total internal energy; m in the second summation runs over all materials in phase φ; h is the specific enthalpy (the difference between h and the specific internal energy, e, accounts for flow work); and H is the non-flow energy source, including the enthalpy of all relevant mass sources in Equation (4.2).

Finally, the equations for pool flow and for atmosphere flow in a flow path are obtained from line integrals of the acceleration equations along a stream line from the center of the *from* volume to the center of the *to* volume. The temporal rate of change of the void fraction, $\partial\alpha/\partial t$, is neglected. The results (in nonconservative form) are expressed by

$$\begin{aligned}\alpha_{j,\varphi}\rho_{j,\varphi}L_j\frac{\partial v_{j,\varphi}}{\partial t} &= \alpha_{j,\varphi}\left(P_i - P_k\right) + \alpha_{j,\varphi}\left(\rho\, g\Delta z\right)_{j,\varphi} + \alpha_{j,\varphi}\Delta P_j \\ &\quad - \frac{1}{2}K^*_{j,\varphi}\alpha_{j,\varphi}\rho_{j,\varphi}\left|v_{j,\varphi}\right|v_{j,\varphi} - \alpha_{j,\varphi}\alpha_{j,-\varphi}f_{2,j}L_{2,j}\left(v_{j,\varphi} - v_{j,-\varphi}\right) \\ &\quad + \alpha_{j,\varphi}\rho_{j,\varphi}v_{j,\varphi}\left(\Delta v\right)_{j,\varphi}\end{aligned} \tag{4.6}$$

where L_j is the inertial length of the flow path; i and k are the "from" and "to" control volumes, respectively, for flow path j; g is the acceleration of gravity; ΔP_j represents any pump head developed in the flow path; K^* is the net form- and wall-loss coefficient; $f_{z,j}$ is the interphase force (momentum exchange) coefficient; $L_{2,j}$ is the effective length over which the interphase force acts (not necessarily equal to the inertial length, see Section 5.5); $\left(\Delta v\right)_{j,\varphi}$ represents the change in velocity through the flow path (the "momentum flux"); and $-\varphi$ denotes the "other" phase relative to φ (atmosphere if φ is pool and vice versa).

Unless a phase is present within at least one of the junction openings associated with a flow path, flow of that phase through that path is impossible and the corresponding flow equation (Equation (4.6)) need not be solved; $v_{j,\varphi}$ is simply set to zero.

The density of a phase in a flow path is ordinarily taken as the density in the donor volume; the phase densities are evaluated from Equation (4.4), with a summation over the materials in the atmosphere. In general, the set of flow equations must be solved iteratively (see

Section 4.2) with "donor" redefined, if necessary for each iteration. If a phase is present within only one of the junction openings, so that flow of that phase within that flow path is only possible in one direction, the donor density is taken as that in the only possible donor volume.

The redefinition of a flow path density between iterations as a result of reversal of the associated flow introduces a discontinuity in the equations. We have observed that this can prevent convergence of the solution under some conditions. Therefore, the next-iterate flow path density is taken as

$$\rho_{j,\varphi}^{(i)} = f\rho_{j,\varphi}^{(i-1)} + (1-f)\rho_{j,\varphi}^{d} \tag{4.7}$$

For the first third of the permitted total number of iterations, *f* is taken as zero, resulting in use of a pure donor density. If further iterations are required, *f* is increased linearly from zero to one for the next third of the permitted total number, introducing an increasing degree of averaging into the definition of density. Finally, *f* is taken as one for the last third of the iterations (if such are required), totally eliminating the numerical discontinuity.

The gravitational head term and the loss term are each somewhat complicated, and will be discussed in detail in Sections 5.3 and 5.4, respectively. The accounting for interphase forces represented by $f_{2,j}$ is described in Section 5.5, and the models available for the pump head are presented in Section 5.6. Note that, as written, the volume fraction, α_φ, cancels identically in the equation.

The last term in Equation (4.6), $v_{j,\varphi}(\Delta v)_{j,\varphi}$, represents the advection of momentum through the flow path, and arises from integration of the term $v(\partial v / \partial x)$ in the continuum equations. The formulation presented here is essentially one-dimensional; in more general geometry, *v* in Equation (4.6) may be interpreted as the velocity component in the direction of flow (denoted by "*x*"); however, the treatment will be incomplete because the cross terms arising from $v_y(\partial v_x / \partial_y)$ are not included in the equations.

By default, even the diagonal momentum flux term in Equation (4.6) is neglected in the solution of the hydrodynamic equations in MELCOR. This is consistent with omission of the kinetic energy in Equation (4.5). These terms (momentum flux and kinetic energy) have traditionally been sources of difficulty in control volume codes because they involve a volume-centered velocity, which requires a multi-dimensional formulation for proper definition. (Note that codes such as RELAP5 [7] make very specific geometric assumptions concerning the relationship between control volumes and flow paths.) The neglected terms in both equations are of order Ma^2, where Ma is the Mach number based on volume-centered velocities, and are ordinarily small (although they may be important for flow boiling with large density gradients). Velocities in flow paths may be sonic or near sonic, but constancy of $h + 1/2v^2$ for adiabatic (not necessarily isentropic) flow assures

that only volume-centered velocities appear in the equations. Choking is treated as an imposed limit on flows based on correlations (see Section 6.4). In any case, consistent inclusion of the v^2 terms would require a proper definition of a volume-centered velocity, including multidimensional effects, and it is clear that this can be done in anything but a full finite difference code (see Section (6.5)). In most cases, no difficulties will arise if MELCOR pressures and enthalpies are considered to be stagnation pressures and stagnation enthalpies.

4.2 Finite Difference Equations

The ordinary differential equations presented in Section 4.1 are converted to linearized-implicit finite difference equations for solution in MELCOR.

For each timestep, Δt , the new (end-of-step) velocities are used in the advection (flow) terms in the mass and energy equations to write

$$M_{i,m}^{n} = M_{i,m}^{o} + \sum_{j} \sigma_{ij} \alpha_{j,\varphi}^{n} \rho_{j,m}^{d} v_{j,\varphi}^{n} F_j A_j \Delta t + \delta M_{i,m} \tag{4.8}$$

$$E_{i,\varphi}^{n} = E_{i,\varphi}^{o} + \sum_{j} \sigma_{ij} \alpha_{j,\varphi}^{n} \left(\sum_{m} \rho_{j,m}^{d} h_{j,m}^{d} \right) v_{j,\varphi}^{n} F_j A_j \Delta t + \delta H_{i,\varphi} \tag{4.9}$$

where superscripts *n* and *o* refer to the new and old time levels, respectively; and δM and δH are the net external sources (integrals from t^o to $t^o + \Delta t$).

The time levels on the donor properties are not explicitly shown in Equations (4.8) and (4.9); they are essentially old values (at t^o), but see the further discussion in Section 4.4.

It is clear that this formulation is conservative with respect to both masses and internal energies because every term representing a flow transfer *from* a volume is exactly balanced by a transfer *to* the volume at the other end of the flow path. Therefore, masses and energies are conserved to within the accumulation of roundoff on the computer used.

In the interest of numerical stability, linearized-implicit ("semi-implicit") differencing is used in several terms in the momentum equation (Equation (4.6)). Specifically, the equation is differenced using projected end-of-step pressures and heads in the acceleration terms, and end-of-step velocities in the frictional loss and momentum exchange terms. Because of the nonlinearity of the frictional loss term, the resulting finite difference equation must be solved iteratively. (Because of nonlinearity of the equation of state used to project the end-of-step pressures, a further iteration may be required. We will return to this in Section 4.3.) We will first discuss the treatment of velocities and then define and discuss the other terms in the finite difference equation.

At each velocity iteration, the form- and wall-loss term is linearized about the best available estimate of v^n, denoted v^{n-} (this is initially v^o), to obtain the finite difference equation for the estimated new, end-of-step velocity:

$$v_{j,\varphi}^{n} = v_{j,\varphi}^{o+} + \frac{\Delta t}{\rho_{j,\varphi} L_j}\left(P_i^{\tilde{n}} + \Delta P_j - P_k^{\tilde{n}} + (\rho\, g\Delta z)_{j,\varphi}^{\tilde{n}} + v_{j,\varphi}^{o}(\rho\,\Delta v)_{j,\varphi}^{o}\right)$$
$$- \frac{K_{j,\varphi}^{*}\Delta t}{2L_j}\left(\left|v_{j,\varphi}^{n-}\right| v_{j,\varphi}^{n} + v_{j,\varphi}'\left|v_{j,\varphi}^{n}\right| - \left|v_{j,\varphi}'\right| v_{j,\varphi}^{n-}\right) - \frac{\alpha_{j,-\varphi} f_{2,j} L_{2,j}\Delta t}{\rho_{j,\varphi} L_j}\left(v_{j,\varphi}^{n} - v_{j,-\varphi}^{n}\right) \qquad (4.10)$$

The nature of the linearization in velocity is determined by the choice of v'. For the first iteration, v' is taken as v^o, giving a tangent (Taylor series) linearization. For later iterations, it is taken as v^{n-} from the previous iteration if the velocity did not reverse during that iteration, or as zero otherwise. The result is to approximate v^2 by the secant from the latest iterate through the next oldest iterate or by the secant through the origin, respectively. Note that the interphase force term is fully implicit with respect to velocities, and that the length over which this force acts, $L_{2,j}$, may differ from the inertial length of the flow path, L_j. See discussion for definition of $P^{\tilde{n}}$.

The superscript "*o*+" on the velocity on the right-hand side of Equation (4.10) indicates that it has been modified from the old value to account for changes in the flow-path void fraction, as discussed below. This was found necessary to prevent initiation of a nonphysical transient whenever the motion of a pool surface through a small junction opening produced a major change in void fraction during a single timestep.

The problem is that the old velocities, v^o, were computed with the old void fraction, α^o; with α^n, they may correspond to a quite different flow state, both in mass flow and in total volumetric flow. This may require large accelerations (and pressure differentials) to maintain the "correct" flow. The cause is, in part, that the time derivative of the void fraction does not appear in the momentum equation. (There are no further problems involving the time level of data on which α is based, and the fact that its treatment is not numerically implicit.)

The definition of "void fraction" in MELCOR is necessarily much more complicated than in a simple fine-zoned finite difference code, and an attempt to include $\partial\alpha/\partial t$ in the momentum equation seemed unlikely to be productive. Therefore, we have chosen to employ an *ad hoc* modification of the "old" velocities to account for changes in void fractions. (Sensitivity coefficient 4408 may be used to disable this modification.) The criteria used are preservation of the total volumetric flux, expressed by

$$\alpha_{j,A}^{n} v_{j,A}^{o+} + \alpha_{j,P}^{n} v_{j,P}^{o+} = \alpha_{j,A}^{o} v_{j,A}^{o} + \alpha_{j,P}^{o} v_{j,P}^{o} \qquad (4.11)$$

and preservation of the relative velocity between the phases, expressed by

$$v^{o+}_{j,A} - v^{o+}_{j,P} = v^{o}_{j,A} - v^{o}_{j,P} \tag{4.12}$$

This results in

$$v^{o}_{j,\varphi} = v^{o}_{j,\varphi} + \left(\alpha^{o}_{j,A} - \alpha^{n}_{j,A}\right)\left(v^{o}_{j,A} - v^{o}_{j,P}\right) \tag{4.13}$$

It is interesting to note that there is an analogous relationship implicit in drift-flux codes. In such codes, the total mass flux (momentum density) is determined by a single momentum equation for each flow path, and a constitutive relation (the drift flux correlation) is then used to partition this flux into liquid and vapor components as a function of void fraction. Thus, when a new void fraction is computed at the start of a timestep, the total mass flux is preserved but the individual phase velocities and the total volumetric flux are not. MELCOR calculations more often involve quasi-steady flows than pressure waves; therefore, preservation of the volumetric flow rather than the momentum density (mass flux) was chosen as the default treatment. (Note that there is no way that both the mass fluxes and volumetric flows could be preserved as the void fraction changes.)

As noted previously, the momentum flux term, $v(\rho\,\Delta v)$ in Equation (4.10), will be omitted by default. We have found no need for implicit treatment of this term if it is included; therefore, start-of-step velocities are used in its evaluation. If the term is to be included in the momentum equation for flow path *j*, the user is required to specify on input record FLnnnMx the flow paths that are logically upstream and downstream from flow path *j*, as described in the FL Users' Guide. The specification of "no such flow path" is permitted, to allow treatment of a flow path connected to a dead-end volume or to one with no other appropriately oriented connection.

The term $(\rho\,\Delta v)$, representing a spatial difference in momentum density, is treated as a donored quantity. It is evaluated based on the direction of flow through flow path *j*, as

$$(\rho\,\Delta v)^{o}_{j,\varphi} = \begin{cases} \rho_i \left(\dfrac{F_{j-} A_{j-} v^{o}_{j-,\varphi}}{A_i} - \dfrac{F_j A_j v^{o}_{j,\varphi}}{A_k} \right) & v^{o}_{j,\varphi} \geq 0 \\ \rho_k \left(\dfrac{F_j A_j v^{o}_{j,\varphi}}{A_i} - \dfrac{F_{j+} A_{j+} v^{o}_{j+,\varphi}}{A_k} \right) & v^{o}_{j,\varphi} < 0 \end{cases} \tag{4.14}$$

Here, subscripts *i* and *k* denote the donor and acceptor volumes, respectively; A_i and A_k are the corresponding user-defined flow areas for these volumes *in the direction of flow*

appropriate to flow path j; and subscripts *j-* and *j+* refer to the designated flow paths that are logically upstream and down stream of *j*, and must connect to volumes *i* and *k*, respectively.

The area ratios in Equation (4.14) serve to convert the momentum density in each flow path to corresponding densities at the volume center, under the assumption of incompressible flow. The volume areas, which may differ from those used in the control volume velocity calculation, must be specified by the user on record FLnnnMk. This allows more accurate description of the actual flow geometry. For example, most of the momentum of a small jet entering a large room will be dissipated close to the point of entry, leaving little momentum to be advected through a second flow path and, in general, this effect will be captured through the ratio of the small flow path area to the large volume area. However, if the two flow paths are closely aligned, so that a fluid jet from one will be captured by the other, the user may capture the effect by specifying a volume flow area appropriate for the jet.

If either flow path *j-* or *j+* is absent (as defined by user input), the corresponding term in Equation (4.14) is neglected, which is equivalent to setting the associated flow path area to zero.

As noted previously, the pressures, $P^{\tilde{n}}$, used in the acceleration terms in Equation (4.10) are *predicted* end-of-step pressures; they are calculated from the linearization of the equation of state about a reference point (denoted by "*") as

$$P_i^{\tilde{n}} = P_i^* + \sum_m \frac{\partial P_i^*}{\partial M_{i,m}} \left(M_{i,m}^n - M_{i,m}^* \right) + \frac{\partial P_i^*}{\partial E_{i,P}} \left(E_{i,P}^n - E_{i,P}^* \right) + \frac{\partial P_i^*}{\partial E_{i,A}} \left(E_{i,A}^n - E_{i,A}^* \right) \tag{4.15}$$

The choice of the linearization point will be discussed in detail in Section 4.3.

The static head terms, $(\rho\, g\Delta z)^{\tilde{n}}$, are also predicted values at end-of-step. However, only changes in pool mass and hydrodynamic volume are included in the projection, with changes in atmosphere mass and phase densities neglected. Specifically,

$$(\rho\, g\Delta z)_{j,\varphi}^{\tilde{n}} = (\rho\, g\Delta z)_{j,\varphi}^{o} + \frac{\partial (\rho\, g\Delta z)_{j,\varphi}}{\partial M_{i,P}} \left(M_{i,P}^n - M_{i,P}^{o+} \right) + \frac{\partial (\rho\, g\Delta z)_{j,\varphi}}{\partial M_{k,P}} \left(M_{k,P}^n - M_{k,P}^{o+} \right) \tag{4.16}$$

In this equation $M_{i,P}^{o+}$ is the mass of pool which can be accommodated below the former elevation of the pool surface at the old pool density. It differs from $M_{i,p}^{o}$ only if there has been a change in the volume/altitude table resulting from a change of virtual volume in control volume *i*. In this case, the difference accounts for the change in pool surface elevation—and therefore in static head—in the absence of a change in pool mass.

The new masses and new energies in Equations (4.15) and (4.16) are given by Equations (4.8) and (4.9), respectively. The derivatives $\partial P / \partial M$ and $\partial P / \partial E$ are calculated by the CVT package, and represent the linearized effect of changing mass and energy contents of the control volumes. See the CVT Reference Manual for further details. The derivatives $\partial(\rho\, g\Delta z)/\partial M$ reflect the linearized effect of changing pool mass on the flow-path head terms; they are defined in Section 5.3.

When all terms associated with each flow are collected together for a given volume, the projected new pressure in Equation (4.15) has the form

$$P_i^{\tilde{n}} = \hat{P}_i + \sum_{s,\Psi} \frac{\partial P_i}{\partial V_{s,\psi}} \sigma_{is} \alpha_{s,\psi} F_s A_s v_{s,\psi}^n \Delta t \tag{4.17}$$

where

$$\begin{aligned} \hat{P}_i = P_i^* &+ \sum_m \frac{\partial P_i^*}{\partial M_{i,m}} \left(\hat{M}_{i,m} - M_{i,m}^* \right) \\ &+ \frac{\partial P_i^*}{\partial E_{i,P}} \left(\hat{E}_{i,P} - E_{i,P}^* \right) + \frac{\partial P_i^*}{\partial E_{i,A}} \left(\hat{E}_{i,A} - E_{i,A}^* \right) \end{aligned} \tag{4.18}$$

$$\hat{M}_{i,m} = M_{i,m}^o + \delta M_{i,m} \tag{4.19}$$

$$\hat{E}_{i,\varphi} = E_{i,\varphi}^o + \delta H_{i,\varphi} \tag{4.20}$$

and

$$\frac{\partial P_i}{\partial V_S} = \sum_m \frac{\partial P_i^*}{\partial M_{i,m}} \rho_{S,m}^d + \frac{\partial P_i^*}{\partial E_{i,P}} (\rho\, h)_{S,P}^d + \frac{\partial P_i^*}{\partial E_{i,A}} (\rho\, h)_{S,A}^d \tag{4.21}$$

Here "S" is used as an abbreviation for "s,ψ", *and*

$$(\rho\, h)_{S,\varphi}^d \equiv \sum_{m\, in\, \varphi} \rho_{S,m}^d h_{S,m}^d \tag{4.22}$$

Because donor densities are used in the advection terms, they appear in the definition of $\partial P / \partial V$ in Equations (4.21) and (4.22). Therefore, $\partial P / \partial V$ depends on the direction of flow. In general, if s,ψ represents a pool (atmosphere) flow, only the pool (atmosphere) energy and materials will be associated with non-zero densities in the evaluation of $\partial P_i / \partial V_{s,\psi}$. However, the code is written with the greater generality of allowing atmosphere (pool) materials to be associated with pool (atmosphere) flows, and different donor density arrays are used to describe flows entering and leaving a flow path. This allows some interactions to be treated as occurring within a flow path. This capability is currently used in conjunction with the SPARC model, as described in Section 6.1.

Substitution of the predicted pressures and heads into the velocity equation leads to a set of linear equations to be solved for the new velocities:

$$\left(1+\frac{K^*_{j,\varphi}\Delta t}{2L_j}\left|v^{n-}_{j,\varphi}+v'_{j,\varphi}\right|+\frac{\alpha_{j,-\varphi}f_{2,j}L_{2,j}\Delta t}{\rho_{j,\varphi}L_j}\right)v^n_{j,\varphi} \;-\; \frac{\alpha_{j,-\varphi}f_{2,j}L_{2,j}\Delta t}{\rho_{j,\varphi}L_j}v^n_{j,-\varphi}$$
$$+\sum_{s,\psi}C(j,\varphi:s,\psi)v^n_{s,\psi}$$

$$= v^{o+}_{j,\varphi}+\frac{K^*_{j,\varphi}\Delta t}{2L_j}\left|v'_{j,\varphi}\right|v^{n-}_{j,\varphi}+\frac{\Delta t}{\rho_{j,\varphi}L_j}\left(\hat{P}_i+\Delta P_j-\hat{P}_k\right)$$
$$+\left(\rho\, g\Delta z\right)^o_{j,\varphi}+\frac{\partial\left(\rho\, g\Delta z\right)_{j,\varphi}}{\partial M_{i,P}}\left(\hat{M}^o_{i,P}-M^{o+}_{i,P}\right) \qquad (4.23)$$
$$+\frac{\partial\left(\rho\, g\Delta z\right)_{j,\varphi}}{\partial M_{k,P}}\left(\hat{M}^o_{k,P}-M^{o+}_{k,P}\right)\Bigg]$$

The summation on the left-hand side is over both phases, ψ, in all flow paths, *s*, although only those paths which connect either to volume *i* or to volume *k* contribute, as will be seen below. The coefficients in the sum are given by

$$C(j,\varphi:s,\psi)=\frac{(\Delta t)^2}{\rho_{j,\varphi}L_j}\alpha_{s,\psi}A_sF_s \left\{-\sigma_{is}\left[\frac{\partial P_i}{\partial V_{s,\psi}}+\delta_{\psi P}\rho^d_{s,P}\frac{\partial(\rho\, g\Delta z)_{j,\varphi}}{\partial M_{i,P}}\right] +\sigma_{ks}\left[\frac{\partial P_k}{\partial V_{s,\psi}}+\delta_{\psi P}\rho^d_{s,P}\frac{\partial(\rho\, g\Delta z)_{j,\varphi}}{\partial M_{k,P}}\right]\right\} \tag{4.24}$$

where

$$\delta_{ij}=\begin{cases}1 & i=j\\ 0 & i\neq j\end{cases} \tag{4.25}$$

by the Kronecker delta. Because of the appearance of σ_{is} and σ_{ks}, the coefficient given by Equation (4.24) is non-zero only for flow paths which connect to volume *i* or to volume *k*; because of the appearance of $\delta_{\psi P}$, the head term appears only in cases where s,ψ is a pool flow.

Equation (4.24) could be made somewhat more compact by obtaining the two sets of terms on the right (for volumes *i* and *k*) from a sum over *all* volumes with appropriate coefficients to pick out the desired terms with the correct signs and eliminate the contributions of all others. However, this would only further conceal the essential point that two flows are coupled by the matrix if and only if there is a volume to which both connect, allowing each flow to affect the pressure differential driving the other.

As mentioned previously, the nonlinearity of the loss (friction) terms and the possibility of flow reversals affecting donor quantities require that the solution of the set of linear Equations (4.23) be repeated until all the new velocities have converged. The control of this iteration is described in Section 4.3.

4.2.1 Inclusion of Bubble-Separation Terms within the Implicit Formulation

To this point, only the contribution of advection terms has been treated within a numerically implicit formulation. The effects of all sources were included in the δM and δH terms in Equations (4.8) and (4.9), which are then treated explicitly. These sources were considered to include several processes that could transfer mass and energy between the pool and atmosphere of a single volume within CHV: condensation/evaporation, bubble separation, and fog deposition. Experience has shown that inclusion of the effects of bubble separation as part of the explicit sources could lead to severe numerical instabilities, particularly in problems involving boiling pools at low pressures. One problem is that the

resulting large oscillations in the calculated elevation of the pool surface resulting from large oscillations in the calculated void (bubble) fraction in the pool can have a significant impact on heat transfer in the COR and HS packages. This was identified as a deficiency in the FLECHT SEASET assessment calculations [8].

The finite difference equations were modified in MELCOR 1.8.3 and later versions to include the transfer of vapor mass and energy from the pool to the atmosphere of a control volume within the implicit formulation. Because bubble separation is an intravolume process, its effects may be included along with those of the equation of state in defining a generalized form of Equation (4.15) in which bubble separation is included *implicitly*, and then eliminated algebraically before proceeding with the solution. The effect is to define net derivatives that include the linearized effect of bubble separation.

The rates of separation of mass and energy by bubbles are primarily functions of the pool void fraction, α, and geometry, and the fact that the observed problems arise from instability in the calculated pool void fraction. We therefore linearize the bubble separation terms within volume i with respect to the pool void fraction in that volume as

$$\delta M_{B,i} = \delta M^*_{B,i} + \frac{\partial\left(\delta M^*_{B,i}\right)}{\partial \alpha_i}\left(\alpha_i^{\tilde{n}} - \alpha_i^*\right) \tag{4.26}$$

$$\delta H_{B,i} = \delta H^*_{B,i} + h_v \frac{\partial\left(\delta M^*_{B,i}\right)}{\partial \alpha_i}\left(\alpha_i^{\tilde{n}} - \alpha_i^*\right) \tag{4.27}$$

where δM^* and δH^* are evaluated using the pool void fraction at the linearization point, α^*, and $\alpha^{\tilde{n}}$ is the projected end-of-step pool void fraction. (The details of the bubble separation model itself will be presented in Section 5.1.3.)

The pool void fraction is a natural function of the specific enthalpy of the pool and the enthalpies of saturated liquid and vapor, and may therefore be considered as a function of the total pool mass, the total pool energy, and the control volume pressure. In response to a variation in these quantities, the change in α is

$$d\alpha_i = \frac{\partial \alpha_i}{\partial M_{i,1}}\left(dM'_{i,1} - dM_{B,i}\right) + \frac{\partial \alpha_i}{\partial E_{i,P}}\left(dE'_{i,P} - h_v dM_{B,i}\right) + \frac{\partial \alpha_i}{\partial P_i} dP_i \tag{4.28}$$

where the primes denote changes in addition to bubble separation, i.e., other sources and advection. Using the same convention, the linearization of the volume pressure (from which Equation (4.15) was derived) becomes

$$dP_i = \sum_m \frac{\partial P_i^*}{\partial M_{i,m}} \left(dM'_{i,m} - \delta_{m1} dM_{B,i} + \delta_{m3} dM_{B,i} \right) + \frac{\partial P_i^*}{\partial E_{i,P}} \left(dE'_{i,P} - h_v dM_{B,i} \right) + \frac{\partial P_i^*}{\partial E}_{i,A} \left(dE'_{i,A} + h_v dM_{B,i} \right) \tag{4.29}$$

Equation **Error! Reference source not found.** can be used to eliminate $dM_{B,i}$ from Equations (4.28) and (4.29), and the resulting equations solved for ∂P_i and $\partial \alpha_i$ as linear functions of the variables $\partial M'_{i,m}$ and $\partial E'_{i,\varphi}$. The results take the form

$$dP_i = \sum_m \frac{\partial P_i^*}{\partial M'_{i,m}} dM'_{i,m} + \frac{\partial P_i^*}{\partial E'_{i,P}} dE'_{i,P} + \frac{\partial P_i^*}{\partial E'_{i,A}} dE'_{i,A} \tag{4.30}$$

$$d\alpha_i = \sum_m \frac{\partial \alpha_i^*}{\partial M'_{i,m}} dM'_{i,m} + \frac{\partial \alpha_i^*}{\partial E'_{i,P}} dE'_{i,P} + \frac{\partial \alpha_i^*}{\partial E'_{i,A}} dE'_{i,A} \tag{4.31}$$

Here the modified pressure derivatives are

$$\frac{\partial P_i^*}{\partial X'} = \frac{\dfrac{\partial P_i^*}{\partial X} - C_i \left(\dfrac{\partial \alpha_i^*}{\partial M_{B,i}} \dfrac{\partial P_i^*}{\partial X} - \dfrac{\partial P_i^*}{\partial M_{B,i}} \dfrac{\partial \alpha_i^*}{\partial X} \right) \Delta t}{1 - C_i \left(\dfrac{\partial \alpha_i^*}{\partial M_{B,i}} + \dfrac{\partial \alpha_i^*}{\partial P_i} - \dfrac{\partial P_i^*}{\partial M_{B,i}} \right) \Delta t} \tag{4.32}$$

where dX' represents any of the variables $dM'_{i,m}$ and $\partial E'_{i,\varphi}$, and

$$\frac{\partial \alpha_i^*}{\partial M_{B,i}} \equiv -\left(\frac{\partial \alpha_i^*}{\partial M_{i,1}} + h_v \frac{\partial \alpha_i^*}{\partial E_{i,P}} \right) \tag{4.33}$$

$$\frac{\partial P_i^*}{\partial M_{B,i}} \equiv \left(\frac{\partial P_i^*}{\partial M_{i,3}} + h_v \frac{\partial P_i^*}{\partial E_{i,A}} \right) - \left(\frac{\partial P_i^*}{\partial M_{i,1}} + h_v \frac{\partial P_i^*}{\partial E_{i,P}} \right) \tag{4.34}$$

are convenient combinations of the derivatives in Equations (4.28) and (4.29).

The momentum equation is constructed and solved as before, but now using Equation (4.30) to project the new pressures. The only differences that result are that the derivatives

$\partial P^* / \partial X'$ appear in Equations (4.18) and (4.21) rather than $\partial P^* / \partial X$, and that only δM^* and δH^* from Equations (4.26) and **Error! Reference source not found.** are included in the source terms in Equations **Error! Reference source not found.** and (4.20). During the solution, any change in bubble separation will be implicitly included by virtue of the modified pressure derivatives.

Once the new velocities are determined, the contribution of advection to new mass and energy inventories (the sums over flow paths in Equations (4.8) and (4.9)) is determined as before. The additional mass and energy transfers resulting from the implicit change in bubble separation in Equations (4.26) and **Error! Reference source not found.** must also be included—in addition to δM^* and δH^*—in defining the new mass and energy inventories in Equations (4.8) and (4.9). Once the contribution of advection has been determined, the contribution of implicit bubble separation is evaluated from

$$\begin{aligned}\alpha_i^{\tilde{n}} = \alpha_i^* &+ \sum_m \frac{\partial \alpha_i^*}{\partial M'_{i,m}} \left(\hat{M}_{i,m} + \delta M_{i,m,advect} - M^*_{i,m} \right) \\ &+ \frac{\partial \alpha_i^*}{\partial E'_{i,P}} \left(\hat{E}_{i,P} + \delta H_{i,P,advect} - E^*_{i,P} \right) \\ &+ \frac{\partial \alpha_i^*}{\partial E'_{i,A}} \left(\hat{E}_{i,A} + \delta H_{i,A,advect} - E^*_{i,A} \right)\end{aligned} \tag{4.35}$$

where the derivatives of the pool void fraction are given by

$$\frac{\partial \alpha_i^*}{\partial X'} = \frac{\dfrac{\partial \alpha_i^*}{\partial X} + \dfrac{\partial \alpha_i^*}{\partial P_i} \dfrac{\partial P_i^*}{\partial X}}{1 - C_i \left(\dfrac{\partial \alpha_i^*}{\partial M_{B,i}} + \dfrac{\partial \alpha_i^*}{\partial P_i} \dfrac{\partial P_i^*}{\partial M_{B,i}} \right) \Delta t} \tag{4.36}$$

in analogy with Equation (4.32), with the understanding that $\partial \alpha^* / \partial X$ is zero unless X is M_1 or E_p.

4.3 Solution Strategy

As written, Equation (4.23) represents a set of linear equations for the latest estimates of the new velocities, $v''_{j,\varphi}$, and is solved by use of a standard linear equation solver. The complete solution procedure, however, is iterative on two levels. As already mentioned, the code requires convergence of the velocity field, so that the velocities $v''^{-}_{j,\varphi}$ used in the loss terms in Equation (4.23) are acceptably close to the new velocities $v''_{j,\varphi}$ found by

solution of these equations. This will, in general, involve iteration. In addition, the code requires that the final new pressures and pool void fractions, P^n and α^n, found from the full equation of state for the new masses and energies (Equations (4.8) and (4.9)) agree well with the linearly projected new pressures and void fractions, $P^{\tilde{n}}$ and $\alpha^{\tilde{n}}$, given by Equations (4.17) and (4.35). Once again, iteration may be required, this time on the definition of the point (denoted by "*") about which pressure is linearized in Equation (4.15).

In general, the advancement of the hydrodynamic equations proceeds as shown in Figure 4.1 (details will be presented after the general approach has been described).

If either iteration fails to converge, the solution attempt is abandoned, the timestep, Δt is reduced, the external sources are redefined appropriately, and the entire procedure repeated starting from the original "old" state. As has already been intimated, and will be discussed in detail in Section 4.5, the thermal-hydraulic packages (CVH and FL) may "subcycle", i.e., several successive advancements may be used to advance the thermal-hydraulic solutions through a full MELCOR system timestep. In general, repetition of the solution with a reduced timestep will affect only a subcycle, and will be restricted to the hydrodynamic packages. Sources will be redefined under the assumption that external source rates are constant over a system timestep. If the resulting subcycle timestep would be excessively small with respect to the system step, CVH will call for a MELCOR fallback with *all* packages required to repeat their calculations with a reduced *system* timestep.

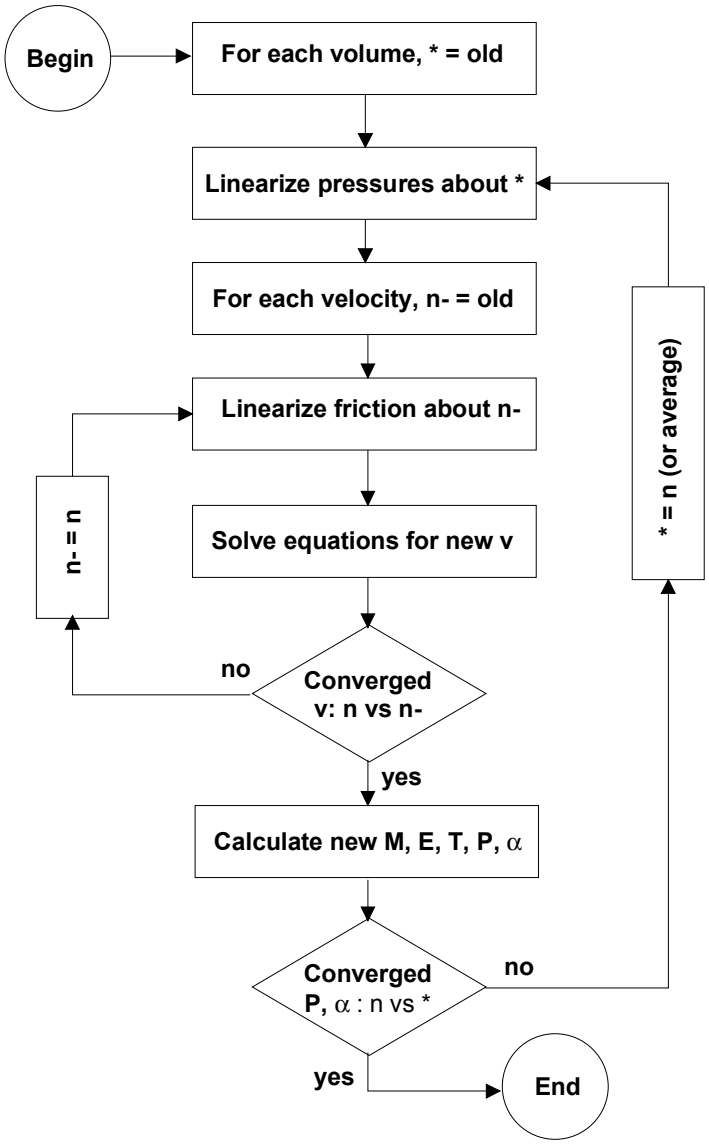

Figure 4.1 Solution of Hydrodynamics Equations

In order to avoid problems with coupling to other packages in MELCOR, large changes in conditions are not permitted to occur during a single system timestep. If any excessive change is observed after the advancement through a system timestep has been completed, the solution is abandoned, and CVH calls for a MELCOR system fallback.

The remainder of this section expands on the general outline given above, discusses special cases, and includes specific details such as convergence criteria.

In the inner (velocity) iteration, the solution of Equation (4.23) is repeated until the new velocities have converged. Convergence requires that no velocity has reversed with respect to the direction assumed in defining quantities, and that no velocity has changed

in magnitude by more than 9% compared to the value that was used in linearizing the friction terms. (The latter criterion is coded using an absolute tolerance and a relative tolerance included as sensitivity coefficients in array C4401.) Note that the relatively loose tolerance on magnitudes affects *only* friction terms; conservation of mass and energy is assured by the form of the equations. Our experience has shown that tightening the convergence criterion affects only the details of very rapid transients, which are of little significance in typical MELCOR calculations.

At each iteration, the friction terms are updated, replacing the velocity, v^{n-}, about which they are linearized by the latest iterate, v^{n}, for flows which have not converged. If one or more of the new velocities has reversed with respect to the direction assumed in defining donor quantities, these quantities are also redefined to reflect the correct flow direction. If there are no flow reversals, new velocities will also be accepted if the corresponding volumetric flows have converged (subject to the same tolerances), starting with the second iteration. The user may also require that after a number of iterations specified by sensitivity coefficient C4401(4) new velocities will be accepted—even if they have not converged to the stated tolerance—if the projected new pressures, $P^{\tilde{n}}$, have converged within 0.05% (comparing successive velocity iterations). The current default is not to accept convergence on this basis.

In some cases, a phase (pool or atmosphere) is available within the junction opening height at only one end of a flow path, and its flow is therefore possible in one direction only. If the donoring assumed in construction of Equation (4.23) makes such a flow "impossible," the corresponding momentum equation is still carried as part of the equation set, but with its coupling to predicted new pressures eliminated by setting the contribution to new mass and energy inventories to zero in Equations (4.8) and (4.9). Therefore, a calculated "impossible" flow has no effect on "real" flows, but its sign indicates the direction the flow would take (if possible) in response to projected end-of-step pressures. If the sign indicates that the calculated new flow remains impossible, the flow will be set to zero. If the sign is reversed—and the flow is therefore possible—the equations must be re-solved with the assumed donor definition reversed.

If the iteration fails (either by exceeding the permitted number of iterations, or by entering an invalid region of the equation of state defined by the CVT package), the entire set of equations is reformulated with a shorter timestep and re-solved. In general, this is handled within the CVH/FL package by subcycling, rather than by calling for a fallback and a reduction of the MELCOR timestep.

After the new velocities are determined (by convergence of the iterative solution to the finite difference equations), they are used to update the masses and energies in the control volumes through Equations (4.8) and (4.9); in the process, the masses moved by flows are limited to the contents of the donor control volumes. While the mass, momentum, and energy equations could be solved simultaneously, this procedure assures that mass and energy are conserved as accurately as possible. Final end-of-step pressures and pool void

fractions, P^n and α^n, corresponding to the new masses and energies are now evaluated using the full nonlinear equation of state. If the discrepancy between P^n and $P^{\tilde{n}}$ or α^n and $\alpha^{\tilde{n}}$ in one or more volumes is too great, the entire iterative solution of the momentum equation is repeated (for a maximum of six times), with a modified definition of the point (denoted by "*") about which the equation of state is linearized (described later). The general criterion for convergence of pressure is agreement of P^n and $P^{\tilde{n}}$ within 0.5% (coded as a sensitivity coefficient C4408(2)). This is tightened to 0.1% if there is no pool in the control volume, and relaxed to 1.0% if there is no atmosphere. The criterion for convergence of pool void fraction is agreement of α^n and $\alpha^{\tilde{n}}$ within 1.0% (coded as a sensitivity coefficient C4412(1)). If the outer iteration fails to converge within this tolerance, the subcycle timestep is cut.

The acceptable discrepancy between projected and actual new pressures should *not* be viewed simply as an accuracy tolerance for pressures; it comes into play only when conditions change sufficiently during a timestep that the nonlinearity of the equation of state becomes significant. For example, a large discrepancy between the projected and actual new pressures in a control volume can arise if the state in the volume has crossed the saturation line, going from saturated conditions ($\partial P/\partial M$ relatively small) to subcooled conditions ($\partial P/\partial M$ very large), or vice versa. It can also occur if there has been a change in the hydrodynamic volume (reflecting relocation of virtual volume), as a result of the omission of the term $(\partial P/\partial V)\delta V$ in writing Equation (4.15). In either case, a projection over the entire timestep is invalid. Therefore, in the outer (pressure) iteration, the linearization point is taken as the best available estimate of the "new" state. On the first iteration, it is the "old" state "o"; on subsequent iterations, it is the latest "new" solution. This is illustrated (in a nonrigorous way) by Figure 4.2, which shows the connection to a conventional Newton iteration for a single-variable problem. After the third iteration the linearization point is defined as the *average* of the last two "new" solutions.

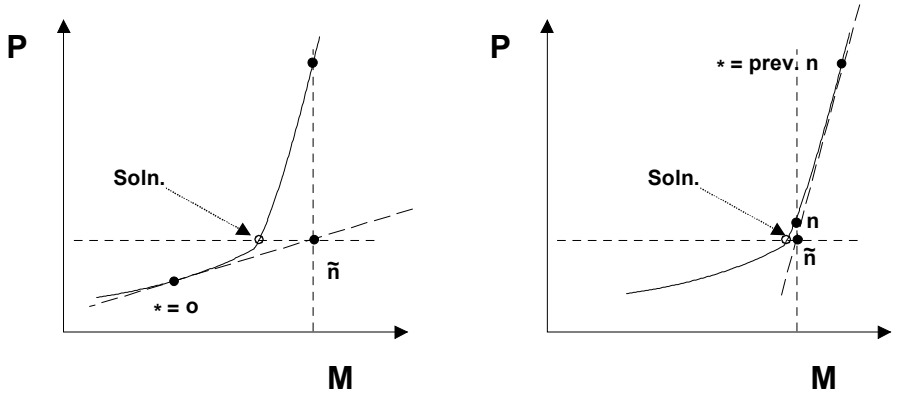

Figure 4.2 Linearization of Pressure vs. Mass

There is a slight subtlety in the redefinition of the linearization point because the PdV work done by the pool on the atmosphere (or vice versa) in a nonequilibrium volume is calculated in CVT rather than in CVH (note that it does not appear in Equation (4.9)).

$$W = P_i^o \left(V_P^o - V_P^n \right) \tag{4.37}$$

based on the old (start-of-step) volume, will be transferred from the atmosphere to the pool in CVT. Therefore, if the new results *returned* by CVT are $M_{i,m}''$, $E_{i,\varphi}''$, and P_i^n, and that solution is rejected, the work must be subtracted from these results to define conditions about which the equations may be linearized. That is, if a solution is rejected, the new linearization point is taken as

$$\begin{aligned} M_{i,m}^* &= M_{i,m}^n \\ E_{i,P}^* &= E_{i,P}^n - P_i^o \left(V_P^o - V_P^n \right) \\ E_{i,A}^* &= E_{i,A}^n + P_i^o \left(V_P^o - V_P^n \right) \end{aligned} \tag{4.38}$$

where n denotes the "new" solution returned by CVT. The essential point is that if M^n, E^n, and V^o are sent as nonequilibrium arguments to CVT, an additional PdV work term will be computed, and the pressure and volumes returned will *not* be P^n and V^n. If, on the other hand, the arguments sent to CVT are M^*, E^*, and V^o, the work computed there will balance that subtracted off Equation (4.38), and the desired values, P^n and V^n, *will* be returned.

Note that the choice of the point * should have little effect on the results obtained (if the solution is successful) because, while the predicted new (end-of-step) pressures are used in the flow equation, they are required by the convergence criteria described earlier to agree well with the actual new pressures. Any small variations in the predictions can have only a modest effect on the results. Therefore, the primary effect of the choice of the point * is on the success of the solution procedure; a poor choice can slow or even prevent convergence.

After the thermal-hydraulic state of the system has been advanced through a MELCOR system timestep, which may involve convergence of the entire calculation described above for several CVH subcycles, the new pressures and temperatures in all control volumes are examined to determine if the changes from old values are acceptably small. The criteria are less than 10% change in pressure and less than 20% plus 1 K change in the temperature of each phase containing more than 1% of the mass in the control volume. These are coded as sensitivity coefficients included in the array C4400. If any change exceeds that permitted, a fallback is requested and the calculation repeated with a reduced MELCOR system timestep.

4.4 Definition of Donor Quantities

The preceding discussion concerns only the finite-difference equations and the solution technique. The definition of the donor densities and enthalpies, ρ^d and h^d, in the matrix coefficients on the left-hand side of the set of flow equations is a completely independent question. (Of course, the choice can affect the accuracy and/or the numerical stability of the entire scheme.)

In the conventional approach, donor quantities are start-of-step ("old") values in the volume from which material is moved; thus, they are not affected by sources. This is consistent with the fact that they are not affected by mass or energy removed, e.g., through flow paths—there are no implicit terms in the donor quantities.

In MELCOR, the sources include changes of material identity resulting from chemical reactions in other packages (COR, BUR, and FDI) as well as from phase changes involving boiling/flashing or fog precipitation within the CVH package itself. The existence of negative mass sources can easily lead to the computation of a negative mass contents in a control volume for one or more materials. An example would be a volume where water vapor was consumed by a clad-oxidation reaction and was also allowed to flow out of the volume through flow paths.

One approach to the problem, as employed by HECTR [2], is to retain the conventional donor definition in terms of pre-source conditions, and to use timestep controls to prevent catastrophes. Non-negativity checks on individual material masses are a necessary part of this approach, and negative-mass fix-ups must sometimes be employed.

This does not seem practical for use in MELCOR, where (for example) clad oxidation may be extremely rapid. There may be conditions where, in the "real world," *no* steam leaves the volume where the reaction is taking place. However, if any is present at the start of the timestep, some would be calculated to leave it under the conventional definition of donor properties. Reduction of the timestep to follow the kinetics of the reaction is not a viable solution; all available steam is really consumed, leaving *none* available for flow out of the volume. Therefore, the problem is handled in MELCOR by modification of the donor quantities (mass and enthalpy) to include the effects of mass sources. The treatment of energy sources depends on the mass sources, as described below.

Mass additions are treated as taking place at constant pressure and temperature. This is a reasonable approximation if conditions in the control volume do not change much during a timestep; if conditions *do* change significantly, the timestep (or subcycle step) is too long by definition, and will be cut as a result of other checks. For each noncondensible gas, for liquid water, and for water vapor, constancy of pressure and temperature implies constancy of the specific volume and of the specific enthalpy. Thus, if liquid water and water vapor are considered to be separate materials, donor partial densities and specific enthalpies are unaffected by sources, and only the amount of each material available for flow is changed. In general, a modification of the volume of this material is involved.

Heat sources, as well as the difference between the enthalpy of added materials and the enthalpy that these materials would have at start-of-step conditions, are not included in this definition of donor quantities. For heat sources, this follows conventional practice. For mass sources, we argue that the enthalpy difference is exactly parallel to a simple heat source because "new" material will be mixed and equilibrated with old, and that it should therefore be treated in the same way as a heat source. The effect of this treatment of sources in MELCOR is to restrict the immediate heating effects of *all* sources to the control volumes in which they occur. While far from a rigorous proof of the correctness of our interpretation, it should be noted that all other approaches tried in the development of MELCOR led to violations of the second law of thermodynamics.

In the current coding, the total post-source mass of each material and its total enthalpy at the pre-source temperature and pressures are calculated, together with the corresponding volume of pool, of fog, and of the gaseous atmosphere. These are used to define donor quantities.

As implied above, addition of mass at constant pressure and temperature requires changes in the volume of the pool, of the fog, and/or of the atmosphere, which must be calculated. There is a complication in that temperature and pressure are not sufficient to define the state of saturated (two-phase) water. Thus, internal energy must be considered to determine the quality of water in the pool and the partition of atmospheric water between vapor and fog.

For a mixture of ideal gases, the total volume is given by

$$V = \sum_m \frac{M_m R_m T}{P} \tag{4.39}$$

where M_m is the mass of species m; R_m is the corresponding gas constant, equal to the universal gas constant divided by the molecular weight; T is temperature; and P is pressure.

This equation is applied to the gaseous atmosphere (subscript A) to yield

$$\delta V_A = \sum_m \frac{\delta M_m R_m T_A^o}{P_A^o} \tag{4.40}$$

where the superscript "o" again denotes old (start of step). The gas constant for water vapor is evaluated as

$$R_{H2O} = \frac{P_{A,\mathrm{H2O}}}{\rho^o_{A,\mathrm{H2O}} T^o_A} \tag{4.41}$$

As noted above, temperature and pressure are not sufficient to define the post-source state of two-phase water. It is assumed that sources of atmospheric vapor and fog remain in those fields for the purposes of defining donor densities. Enthalpies and densities corresponding to the start of the advancement step are used if available; otherwise, appropriate saturation properties are assumed. Similarly, pool sources are now treated as having the same mass quality as the pool mass present at the start of the timestep. If there was none, saturated liquid properties at the old (total) pressure are used.

4.5 Timestep Control and Subcycling

As mentioned in previous sections of this Reference Manual, the thermal-hydraulic packages (CVH and FL) are permitted to subcycle. That is, they may employ several successive sub steps to advance the state of the system through a MELCOR system timestep from t^o to $t^n = t^o + \Delta t$. Only the final state (at t^n) becomes part of the MELCOR database.

The code keeps track of the maximum subcycle timestep that it is willing to attempt, $\Delta t_{sub,\max}$. Each attempted advancement starts from the last point successfully reached, t^{last}, with a step given by

$$\Delta t_{sub} = \min\left(\Delta t_{sub,\max}, t^n - t^{last}\right) \tag{4.42}$$

Following a failed attempt, $\Delta t_{sub,\max}$ is reduced by a factor of 2. (The possible reasons for failure of a subcycle were discussed in Section 4.3.) Following a successful advancement, it is reevaluated as

$$\Delta t^n_{sub,\max} = \max\left(\Delta t, 1.6 F \Delta t^o_{sub,\max}\right) \tag{4.43}$$

where F is a factor which allows a faster increase if the convergence of pressures in the outer iteration if the solution of the momentum equation was much closer than required by the tolerance. Specifically,

$$F = \max\left(1, 2 - 10\frac{\left|\varepsilon P/P\right|^o_{\max}}{\left(\varepsilon P/P\right)_{tol}}\right) \tag{4.44}$$

where $\varepsilon P/P$ is the relative error in the predicted pressure (compared to the new pressure); the subscripts "max" and "tol" denote a maximum over volumes and a tolerance, respectively; and the superscript "o" again denotes the previous subcycle. The tolerance is coded as a sensitivity coefficient, part of the array C4408(2), with a default value of 0.005.

If the failure of an attempted advancement results in a subcycle length, Δt_{sub}, which is less than $0.01\,\Delta t$, the timestep is aborted, and the executive level of MELCOR is directed to perform a fallback. That is, the advancement of *all* packages is repeated from t^o with a reduced value of Δt. As currently coded, this reduction is by a factor of 2.

When, as a result of one or more steps, the thermal-hydraulic packages have advanced the state of the system from t^o to t^n, the changes in pressures and temperatures in all control volumes are examined. As mentioned in Section 4.3, a change of more than 10% in pressure, or of more than 20% plus 1 K in the temperature of each phase containing more than 1% of the mass in a control volume, will result in a fallback, where the tolerances are coded as sensitivity coefficients included in the array C4400. As currently coded, the fallback is not performed if the MELCOR system timestep is already within a factor of 2 of the minimum. The change is accepted, and the calculation is allowed to continue.

If these tolerances are met, a maximum acceptable timestep is estimated for the next MELCOR step, such that certain stability and accuracy criteria will (most probably) be met. This estimate considers several factors.

First, changes in pressures and temperatures must be acceptably small. An acceptable step is estimated, based on the rates of change of temperatures and pressures for the just-completed step. For pressures, the change in the pressure of control volume *i* is desired to be no more than $0.0 + 0.05\ P_i^o$. This will (probably) be the case if the timestep, based on pressure change, is not greater than

$$\Delta t_P^n = \min_i \left(\frac{0.0 + 0.05 P_i^o}{\left| P_i^n - P_i^o \right|} \right) \Delta t \qquad (4.45)$$

where *i* includes all control volumes in the problem. Similar limiting timesteps are estimated for changes in temperature, as

$$\Delta t^n_{T_\varphi} = \min_i \left(\frac{1.0 + 0.1 T^o_{\varphi,i}}{\left| T^n_{\varphi,i} - T^o_{\varphi,i} \right|} \right) \Delta t \tag{4.46}$$

where φ is *P* or *A*. If a phase represents less than one percent of the mass in a control volume, it is excluded from these calculations. All of the constants in Equations (4.45) and (4.46) (including the zero) are coded as sensitivity coefficients, included in array C4400, and can be modified by user input if desired. The default values provide a safety factor of two between the desired maximum changes and the changes which will lead to a fallback. Changes in timestep control should be made in parallel with changes in the corresponding fallback criteria.

The (material) Courant condition provides another restriction through the stability requirement that a timestep may not be long enough to permit replacement of all of the material in a volume. (While not a rigorous statement of the condition, this is a workable approximation to it.) This leads to the limitation that the timestep be no greater than

$$\Delta t^n_{Cou} = 0.5 \min_i \left(\frac{V^*_i}{\Delta V_{i,out}} \right) \Delta t \tag{4.47}$$

where V^*_i is the total volume of materials initially in the volume, including mass sources (at the old temperature and pressure, see Section 4.4), and $\Delta V_{i,out}$ is the total volume, pool and atmosphere, moved out of the volume during the timestep. Note that $\Delta V_{i,out}$ accounts for flow *from* volume *i* and flow *to* volume i. The factor of 0.5 is coded as a sensitivity coefficient in the array C4400.

The accuracy of the solution of the momentum equation (as estimated by the linear equation solver) is also considered. It is used to define

$$\Delta t^n_{Mom} = \begin{cases} 0.9 \Delta t & N < 2 \\ (N - 0.9)\, \Delta t & N \geq 2 \end{cases} \tag{4.48}$$

where *N* is the number of significant figures in the velocities, as estimated by the solver. Note: the factor 0.9 is coded as a sensitivity coefficient in array C4400.

Finally, the timestep given by the most restrictive of the desired CVH constraints,

$$\Delta t^n_{CVH} = \min\left(\Delta t^n_P, \Delta t^n_{T_P}, \Delta t^n_{T_A}, \Delta t^n_{Cou}, \Delta t^n_{Mom} \right) \tag{4.49}$$

is chosen as an upper bound on the acceptable timestep and communicated to the executive routines for consideration in setting the next system timestep.

5. Constitutive Relations

5.1 Pool/Atmosphere Mass and Energy Transfer

When equilibrium thermodynamics is used in a control volume, mass and energy transfer between the pool and the atmosphere is implicitly determined by the assumption that the pool and the atmosphere are in thermal and evaporative equilibrium. In this case, CVT performs the transfers which are, effectively, instantaneous.

If a volume in which nonequilibrium thermodynamics is specified contains both a pool and an atmosphere, CVT will not transfer mass between them, and will only transfer energy in the amount of the PdV work done by one on the other. CVH must therefore calculate the energy exchange at the pool surface, the evaporation or condensation, and the phase separation in the pool as bubbles rise and join the atmosphere or as fog settles into the pool. The mass/energy transfer at the pool surface, which is driven by convection and/or conduction, and any phase separation resulting from bubble rise, are treated as two separate processes. The deposition of fog is ordinarily treated by the aerosol dynamics portion of the RN package, but a simple, non-mechanistic limit on fog density, described in Section 5.1.4, is imposed by the CVH package when large fog densities are encountered.

Bubble rise is accounted for only if nonequilibrium is specified. Given the assumption that there are no noncondensible gases in the pool, the equilibrium assumptions prohibit the presence in bubbles in the pool whenever such gases are present. (Total pressure exceeds saturation pressure by the partial pressure of the noncondensible gases. The liquid water is therefore subcooled, and cannot be in equilibrium with a bubble containing only water vapor.) All water vapor in an equilibrium volume is therefore assumed to reside in the atmosphere to avoid a discontinuity in behavior, and the vapor content of the pool is *always* calculated as zero by CVT for equilibrium volumes.

5.1.1 Mass Transfer at the Pool Surface

Calculation of phenomena at the pool surface requires simultaneous solution of the equations of heat and mass transfer. It may be reduced to finding the temperature of the pool surface that satisfies the requirements that

(1) the mass flux (evaporation or condensation) is that given by the mass diffusion equation for the existing gradient in the partial pressure of water vapor between the surface and the bulk atmosphere,

(2) the net heat flux delivered to the interface by convection, conduction, and radiation is equal to the latent heat required by the evaporation or condensation heat flux, and

(3) the partial pressure of water vapor at the pool surface corresponds to saturation at the surface temperature.

In the presence of noncondensible gases, the mass flux, defined as positive for evaporation, is given by

$$\dot{m}'' = C \ln\left(\frac{P_A - P_{w,A}}{P_A - P_{w,I}}\right) \tag{5.1}$$

where P_A is the total pressure; $P_{w,A}$ is the partial pressure of water vapor in the bulk atmosphere; $P_{w,I}$ is the partial pressure of water vapor at the interface; and C is a coefficient.

This equation is also applied in the absence of noncondensibles, requiring only that $P_{w,I} = P_{w,A}$; it will be used in a modified form (Equation (5.6)) in which there is not even the appearance of a singularity.

Using the analogy between mass transfer and heat transfer [9], C is obtained from

$$\frac{C\,L}{\rho_v D} = \frac{h_A L}{k}\left(\frac{Sc}{\mathrm{Pr}}\right)^{1/3} \tag{5.2}$$

where Pr and Sc are the Prandtl and Schmidt numbers given by

$$\mathrm{Pr} = \frac{\mu_A c_{P,A}}{k_A} \tag{5.3}$$

and

$$Sc = \frac{\mu_A}{\rho_A D_{w,A}} \tag{5.4}$$

respectively. In these equations, L is a characteristic length, which cancels in the final result; h is the coefficient of convective heat transfer; ρ_v is the density of saturated water vapor at total pressure; c_P is the specific heat at constant pressure; μ is dynamic viscosity;

k is thermal conductivity; ρ is density; D_w is the mass diffusivity of water vapor; and subscript A refers to the atmosphere.

Properties are calculated for the current bulk atmosphere composition. Density and specific heat are calculated in the CVT package, as described in the Control Volume Thermodynamics (CVT) Package Reference Manual, while the viscosity and thermal conductivity are calculated by the MP package, as described in the Material Properties Package Reference Manual. The general model in the MP package (based on Reference [10], but using the complete composition of the atmosphere) will be used.

Conditions at the interface are assumed to be saturated, thus relating the partial pressure at the interface, $P_{w,I}$, to the temperature there, T_I, through

$$\mathrm{P_{w,I}} = P_{sat}\left(T_I\right) \tag{5.5}$$

If Equation (5.1) is solved for $P_{w,I}$, the inverse of Equation (5.5) may be expressed as

$$\mathrm{T_I} = T_{sat}\left[P_A - \left(P_A - P_{w,A}\right)\exp\left(\frac{-\dot{m}''}{C}\right)\right] \tag{5.6}$$

Simultaneous with mass transfer, there are temperature-driven heat flows from the pool to the surface (interface), Q_{PS}, and from the atmosphere to the surface, Q_{AS}. These do not include mass-transfer effects, and may be approximated by using ordinary heat-transfer correlations. Processes (such as radiation) treated by other packages may also deposit energy directly "in" the surface, at a rate Q_{RS}. The net heat flow to the surface is then related to the evaporation rate by

$$\dot{m} = \frac{Q_{PS} + Q_{AS} + Q_{RS}}{h_{fg}} \tag{5.7}$$

where

$$h_{fg} = h_g - h_f \tag{5.8}$$

is the latent heat of evaporation. In current coding, the enthalpies h_f and h_g are evaluated at bulk conditions for the pool and atmosphere, respectively. (Other interpretations are possible but, in all cases investigated, other choices had no significant effect on calculated results.)

The heat flows, Q_{PS} and Q_{AS}, from the pool and atmosphere to the surface, may both be considered to be proportional to the corresponding temperature differences

$$Q_{PS} = h_P^*(T_P - T_I)A_s \tag{5.9}$$

$$Q_{AS} = h_A^*(T_A - T_I)A_s \tag{5.10}$$

where A_S is the surface area of the pool and the h^* are effective heat transfer coefficients, including radiation within the CVH package, as discussed in Section 5.1.2. This allows Equation (5.7) to be solved for T_I in the form

$$T_I = \frac{h_P^* T_P + h_A^* T_A + \left(Q_{RS} - \dot{m}\, h_{fg}\right)/A_S}{h_P^* + h_A^*} \tag{5.11}$$

Equations (5.6) and (5.11) provide two simultaneous equations for T_I and $\dot{m}$, which are solved iteratively with a bound-and-bisect method. The fact that h_p^*, h_A^* and the mass transfer coefficient C are themselves functions of the interface temperature, T_I, is accounted for during the iteration.

In MELCOR, the rate given by this solution is calculated using start-of-step conditions and is then applied to the entire step, Δt.

The resulting transfers of mass and energy are

$$\Delta M_P = -\dot{m}\Delta t \tag{5.12}$$

$$\Delta E_P = -\left(\dot{m}h_f + Q_{PS}\right)\Delta t \tag{5.13}$$

$$\Delta M_{w,A} = \dot{m}\Delta t \tag{5.14}$$

$$\Delta E_A = -\left(\dot{m}\, h_g - Q_{AS}\right)\Delta t \tag{5.15}$$

If condensation is occurring at a rate that exceeds 90% of the total water vapor in the atmosphere during the timestep, the mass transfer is limited to this value to avoid numerical problems. Equations (5.12) through (5.15) are then recalculated so as to conserve mass and energy. The limiting value is coded as a sensitivity coefficient in array C4407.

The energy transfers are written as internal energies, "ΔE s", because they are added to the internal energy of the material, but are actually enthalpies, "ΔH s". The difference, $P\Delta V$, is later cancelled by the volume work accounted for in calculations in the CVT package. The necessity for this may be seen by considering a case where essentially all of the pool is evaporated; its energy inventory must be decremented by its total *enthalpy* to ensure that the final energy content will be near zero after the work term is accounted for in CVT.

This formulation clearly conserves both mass and energy, with the net heat added to the control volume being

$$\Delta E_P + \Delta E_A = Q_{RS}\Delta t \tag{5.16}$$

as is easily shown from the preceding equations. Note from Equations (5.13) and (5.15) that the use of *bulk* values for h_f and h_g eliminates the possibility of nonphysical cooling of an evaporating subcooled pool or heating of a condensing superheated atmosphere. Other nonphysical results from the explicit numerics are avoided by limiting the sensible heat flow from the pool or atmosphere to the heat content above the interface temperature, as

$$Q_{\varphi S}\Delta t = \min\left[Q^0_{\varphi S}\Delta t, M_\varphi c_{P\varphi}\left(T_\varphi - T_I\right)\right] \qquad \text{if } T_\varphi > T_I \tag{5.17}$$

where M_φ is the phase mass, φ is P or A, and $Q^0_{\varphi S}$ is the value calculated as described in the following section.

5.1.2 Heat Transfer at the Interface

The heat flows at the pool and atmosphere interface (surface) are calculated from

$$Q_{\varphi S} = \left[h_\varphi\left(T_\varphi - T_I\right) + \sigma_B\left(T_\varphi^4 - T_I^4\right)\right]A_S \tag{5.18}$$

where σ_B is the Stefan-Boltzmann constant and all other variables were defined above. Note that view factors and emissivities of unity are assumed in the radiation contributions. The effective heat transfer coefficient, including radiation, is then

$$h^*_\varphi = h_\varphi + \sigma_B\left(T_\varphi^2 + T_I^2\right)\left(T_\varphi + T_I\right) \tag{5.19}$$

The normal heat transfer coefficient, corresponding to convection or conduction in the absence of mass transfer, is defined by

$$h_{\varphi} = \max\left(h_{forced,\varphi}, h_{free,\varphi}, k_{\varphi} / L_{\varphi}\right) \tag{5.20}$$

The forced convection correlation, taken from TRAC [6], is appropriate for horizontal stratified flow:

$$h_{forced,\varphi} = 0.02 \rho_{\varphi} c_{P\varphi} v_{v,\varphi} \tag{5.21}$$

The control-volume average velocity, $v_{v,\varphi}$, is discussed in Section 6.5. The natural convection heat transfer used is taken as the maximum of laminar and turbulent correlations appropriate for horizontal surfaces [11] as

$$h_{free,P} = \max\left[0.27(Gr\,\mathrm{Pr})_P^{1/4}, 0.27(Gr\,\mathrm{Pr})_P^{1/4}\right]\frac{k_P}{X_P} \tag{5.22}$$

$$h_{free,A} = \max\left[0.54(Gr\,\mathrm{Pr})_A^{1/4}, 0.14(Gr\,\mathrm{Pr})_A^{1/3}\right]\frac{k_A}{X_A} \tag{5.23}$$

where the characteristic dimension is

$$X = \min(D_s, L) \tag{5.24}$$

Here *Pr* is the Prandtl number, defined in Equation (5.3), and *Gr* is the Grashof number,

$$Gr = g\,\beta|\Delta T|X^3(\rho/\mu)^2 \tag{5.25}$$

In these equations, in addition to variables previously defined, β is the thermal expansion coefficient; *L* is thickness (depth); *g* is the acceleration of gravity; and D_s is the diameter of the surface.

Note that the absolute value of the temperature difference is used in the Grashof number. Therefore, the same correlation is used for both signs of the temperature gradient, although it is only appropriate for one of them. In fact, the correlations were derived for rather simpler geometries than exist in reactor primary and containment systems. In particular, the effects of other heated or cooled surfaces may well be more important in establishing convection than is the pool surface itself. A recent review of the modeling in MELCOR [12] concluded that “Wall effects are probably sufficiently important and dependent upon geometric details that no general correlation could be constructed.” This

review also compares MELCOR to a number of other codes including TRAC [6], RELAP5 [7], HECTR [2], CONTAIN [3] and MAAP [4], and found that "there is no clearly accepted model. Treatment in the other codes suffers from limitations no less significant than those in MELCOR."

In Equations (5.22) and (5.23), the first expression refers to laminar convection and the second to turbulent. Note that the value for $(Gr\,\mathrm{Pr})$ at the laminar-turbulent transition is implicitly defined such that the heat transfer coefficient is continuous there. All of the numerical constants in Equations (5.21), (5.22), and (5.23) are coded as sensitivity coefficients in the array C4407, and may therefore be modified through user input. In particular, a laminar-turbulent transition may be introduced into the correlation for free convection in the pool even though there is none in the default version of Equation (5.22). The final term in Equation (5.20), *k/L*, is the conduction limit.

5.1.3 Bubble Rise and Phase Separation

Boiling, as a result of heat deposition in the pool, or flashing, in response to a reduction in the pressure of a control volume, may cause vapor bubbles to appear in the pool. As these bubbles rise to the surface, they transport mass and energy from the pool to the atmosphere. In general, the velocity is insufficient to remove all the bubbles, resulting in a two-phase pool.

The bubble rise model in MELCOR is very simple. It assumes steady state with an upward volume flow of bubbles that varies linearly from zero at the bottom of the control volume to a value of J_{max} at the top, and a constant rise velocity, v_o, of 0.3 m/s for the bubbles. This value is approximately correct for typical gas bubbles rising in water under near-atmospheric pressures, where the effect is most important, and is not seriously in error under other conditions. (The rise velocity is coded as a sensitivity coefficient in array C4407.) For a volume of constant cross-sectional area, the assumptions correspond to a uniform generation rate of vapor throughout the volume with no bubbles entering the bottom. Other assumptions would lead to different results, but within roughly a factor of 2 of those presented here.

Under the stated assumptions, the average void fraction and the volume of bubbles which leave the volume during a time Δt are given by

$$\overline{\alpha} = \frac{J_{\max} Z_P}{2 v_0 V_P} \tag{5.26}$$

$$\Delta V_B \equiv V_B^{tot} - V_B^{final} = J_{\max} \Delta t \tag{5.27}$$

where V_P is the total (swollen) volume of the pool; Z_P is the depth; V_B^{tot} is the sum of the initial volume of bubbles and the volume created in the pool as a result of sources during Δt ; and V_B^{final} is the volume of bubbles remaining at the end of the step.

Therefore, since

$$V_B^{final} = \bar{\alpha} V_P \tag{5.28}$$

the average void fraction may be eliminated to show that only a fraction

$$f = \frac{V_B^{final}}{V_B^{tot}} = \frac{1}{1 + 2v_0 \Delta t / Z_P} \tag{5.29}$$

of the bubbles that were in the pool during the timestep will remain after bubble-rise is accounted for.

The total mass of vapor in the pool is calculated as

$$M_{v,P}^{tot} = \frac{h_P - h_l}{h_v - h_l} M_P \tag{5.30}$$

where M_P and h_P are the total pool mass and enthalpy, including the vapor component. The specific enthalpies h_v and h_l correspond to saturated vapor and liquid, respectively, at the pressure of the control volume ($M_{v,P}^{tot}$ is then limited to M_P). In accordance with Equation (5.29), all but a fraction f of this is moved to the atmosphere; if this is insufficient to reduce the average void fraction in the pool to 0.40 or less, additional mass is moved to reach that limit. (This limit is coded as a sensitivity coefficient in array C4407. The default value is the approximate upper limit of the bubbly flow regime [13].) The mass moved takes with it the enthalpy of saturated vapor, h_v. The limit is imposed after sources are accounted for, and again after the entire flow solution for a CVH subcycle has been successfully completed.

5.1.4 Fog Deposition

Fog in MELCOR consists of water droplets suspended in the atmosphere. If the RadioNuclide (RN) package is active, this fog also forms the water component of the aerosol field treated by the MAEROS [14] model, and is subject to various deposition mechanisms. The CVH package has no mechanistic models for fog removal and ordinarily relies on the MAEROS model to calculate these mechanisms. For cases where the RN package is not active, an upper limit (coded as a sensitivity coefficient, C4406(1)) is

imposed on the average density of fog in a control volume atmosphere, and excess fog is removed as "rain." (This procedure will also be followed if the RN package is active but its calculated aerosol removal rate is insufficient to reduce the fog density below the limiting value.) The default value of the limit is 0.1 kg/m^3, is based on the practical upper limit observed in a number of MAEROS calculations. If the fog density in any volume exceeds that limit, the excess is summarily transferred to the pool in that volume. The possibility of such rain is considered after mass sources are added, and again after the entire flow solution for a CVH subcycle has been successfully completed.

5.2 Flow Path Void Fractions

The void fraction assigned to a flow path determines the extent to which it is shared by pool and atmosphere. It will depend in general on the conditions at the ends of the flow path (its junctions with the *from* and *to* control volumes), and on the direction of flow. Input options are provided to allow the user to override the geometrical calculation performed for normal flow paths and enforce preferential flow of pool or atmosphere. These options are discussed below.

5.2.1 Normal Flow Paths

A flow path connects two control volumes; a void fraction can therefore be defined at each junction, based on the fraction of the junction area that lies above the pool surface in the corresponding volume. The void fraction for the *from* connection is calculated as

$$\alpha_{fm} = \frac{z_{TJ,fm} - z_{P,fm}}{z_{TJ,fm} - z_{BJ,fm}} \tag{5.31}$$

where *TJ*, *BJ*, and *P* refer to the top of the junction, the bottom of the junction, and the pool, respectively, and "*fm*" denotes the *from* volume or connection. In effect, the opening is treated as if it were rectangular. The void fraction for the *to* connection is defined similarly.

From these two junction void fractions, a single flow path void fraction must be defined. Unless the flow, based on velocities from the previous iteration in the flow solution, is strictly countercurrent (meaning that pool and atmosphere velocities are non-zero and have opposite signs), the void fraction in the flow path is taken as that at the donor junction. That is, α_j is taken as α_{fm} if the flow is positive and as α_{to} if it is negative. (If there is no flow, so that both velocities are zero, α_j is taken as α_{fm}.)

If the previous-iteration flows are countercurrent, the flow-path void fraction is taken as a weighted average of the junction values,

$$\alpha_j = \frac{\rho_A^{-1/2}|v_A|\alpha_{Ad} + \rho_P^{-1/2}|v_P|\alpha_{Pd}}{\rho_A^{-1/2}|v_A| + \rho_P^{-1/2}|v_P|} \qquad \text{(countercurrent)} \qquad (5.32)$$

where *Ad* and *Pd* refer to the donor junction for atmosphere flow and that for pool flow, respectively. While there is no rigorous basis for this procedure, it is motivated by an analysis of flooding, and also assures continuity in the definition as either velocity passes through zero.

There is a further check for over extraction of the pool from the donor volume. The void fraction is modified if necessary to ensure that the volume of pool which would be moved with the previous iterate velocity, $(1-\alpha_j)|v_P|F_j A_j \Delta t$, does not exceed the total volume of pool above the elevation of the bottom of the flow path opening in the pool-donor volume.

There is a similar check for over-extraction of the atmosphere based on the previous-iteration atmosphere velocity and the volume of atmosphere below the top of the flow path opening. These modifications were introduced to eliminate a number of problems with nonconvergence observed in test calculations.

5.2.2 Pool-First and Atmosphere-First Flow Paths

These options allow preferential movement of pool or atmosphere materials through a flow path. This is accomplished by overriding the normal definition of the void fraction for these flow paths. The void fraction is initially set to 0.0 for a pool-first path and to 1.0 for an atmosphere-first path if the preferred phase is present within the junction opening. This α is then subjected to the pool- or atmosphere-extraction limitation described in the preceding subsection. If the preferred phase is not available, the other phase is permitted to flow in the normal manner.

5.3 Hydrostatic (Gravitational) Heads

The pressure differential acting on phase φ in flow path *J*, connecting control volumes *i* and *k*, was abbreviated in Section 4 at $P_i - P_k + (\rho g \Delta z)_{j,\varphi}$. P_i and P_k are the thermodynamic pressures in control volumes i and k respectively, and correspond to the altitudes of the pool surfaces. The term $(\rho\, g \Delta z)_{j,\varphi}$ contains all gravitational head terms within the control volumes and along the flow path. Figure 5.1 illustrates the elevation changes associated with a flow path.

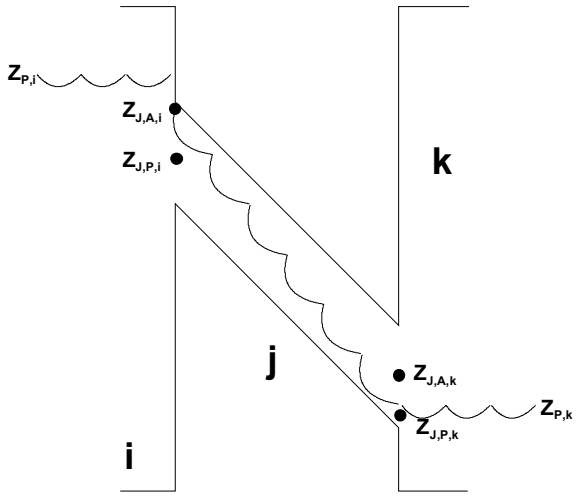

Figure 5.1 Elevations Involved in Gravitational Head Terms

Examination of Figure 5.1 shows that there are three contributions to the gravitational head. The first is the pressure difference between the pool surface at $z_{p,i}$ (where the volume pressure is defined) and that at the average elevation, $z_{J,\varphi,i}$, of the phase in the junction opening in volume *i*

$$\left(P_{J,i} - P_i\right)_\varphi = \begin{cases} \rho_{P,i} g\left(z_{P,i} - z_{J,\varphi,i}\right) & z_{P,i} \geq z_{J,\varphi,i} \\ \rho_{A,i} g\left(z_{P,i} - z_{J,\varphi,i}\right) & z_{P,i} < z_{J,\varphi,i} \end{cases} \tag{5.33}$$

In this equation, the average elevations of the phases in the junction openings are given by

$$z_{J,P,i} = \max\left\{z_{BJ,i}, \frac{1}{2}\left[z_{BJ,i} + \min\left(z_{P,i} + z_{TJ,i}\right)\right]\right\} \tag{5.34}$$

$$z_{J,A,i} = \min\left\{z_{TJ,i}, \frac{1}{2}\left[z_{TJ,i} + \max\left(z_{P,i} + z_{BJ,i}\right)\right]\right\} \tag{5.35}$$

where *BJ* and *TJ* again refer to the top and bottom of the junction opening, as in Section 5.2.

The second contribution to the static head comes from the corresponding pressure difference in volume *k*

$$\left(P_{J,k} - P_k\right)_{\varphi} = \begin{cases} \rho_{P,k} g\left(z_{P,k} - z_{J,\varphi,k}\right) & z_{P,k} \geq z_{J,\varphi,k} \\ \rho_{A,k} g\left(z_{P,k} - z_{J,\varphi,k}\right) & z_{P,k} < z_{J,\varphi,k} \end{cases} \tag{5.36}$$

and the third term is the gravitational head in phase φ along the flow path

$$\left(P_{J,k} - P_{J,i}\right)_{\varphi} = \overline{\rho}_{J,\varphi} g\left(z_{J,\varphi,i} - z_{J,\varphi,k}\right) \tag{5.37}$$

based on the density of that phase in the flow path. The density of a phase in a flow path is taken as the maximum of the volume values,

$$\overline{\rho}_{J,\varphi} = \max\left(\rho^{d}_{J,\varphi}, \rho^{a}_{J,\varphi}\right) \tag{5.38}$$

because use of a donor value would introduce an unacceptable discontinuity in the gravitational head whenever the direction of a flow reversed. The maximum rather than a simple average is used because the value in a volume where the phase is not present may not be well defined.

The net gravitational head term is then defined as the sum of these three contributions:

$$\left(\rho\, g \Delta z\right)_{j,\varphi} = \left(P_{J,i} - P_i\right)_{\varphi} + \left(P_{J,k} - P_{J,i}\right)_{\varphi} - \left(P_{J,k} - P_k\right)_{\varphi} \tag{5.39}$$

Figure 5.1 shows only two of the three possible cases: $z_P > z_{TJ}$ and $z_{TJ} > z_P > z_{BJ}$, but the third $\left(z_{BJ} > z_P\right)$ should be easily visualized.

The derivatives of Equation (5.39) with respect to pool masses at constant densities are required for the implicit projection of the head terms as shown in Equation (4.16). These are then used in the implicit flow equation, Equations (4.23) and (4.24). Under the assumption of constant pool density, we have

$$\frac{\partial}{\partial M_P} = \frac{1}{\rho_P A_P} \frac{\partial}{\partial z_P} \tag{5.40}$$

where A_P is the cross-sectional area of the control volume at z_P (the area of the pool surface). Evaluation of the derivatives is greatly complicated by the fact that $\rho_{i,\varphi}, \rho_{k,\varphi}$, and $\overline{\rho}_{J,\varphi}$ are all potentially different. However, by ignoring this difference and neglecting all terms which contain ρ_A rather than ρ_P, we may obtain the approximate result

$$\frac{\partial(\rho\, g\Delta z)_{j,\varphi}}{\partial M_{P,s}} = \begin{cases} \dfrac{\sigma_{js} g}{A_{P,s}} & z_{P,s} > z_{J,\varphi,s} \\ 0 & z_{P,s} \le z_{J,\varphi,s} \end{cases} \qquad (5.41)$$

where *s* is either *i* or *k*, and σ_{js} provides the appropriate sign. This approximation has been found to be adequate in practice, and is currently employed in MELCOR.

Equation (5.41) may be derived from the preceding equations by performing the indicated derivative under the stated assumptions and approximations. These assumptions and approximations are equivalent to considering only the effect of changes in z_P on the pool contribution to the static head; this observation also allows the equation to be written down by inspection of Figure 5.1.

5.4 Form Loss and Wall Friction

The frictional pressure drops resulting from material flows contain contributions from both form loss and wall friction. The form-loss contribution is based on user-input coefficients; the wall-friction terms are computed within MELCOR, based on segment lengths and roughnesses input by the user. Because a single MELCOR flow path may be used to represent a rather complicated hydraulic path, the wall-friction terms may be computed for a path composed of one or more segments which are connected in series. (As will be noted below, a MELCOR segment may represent a number of parallel pipes.) This approach may also be used to approximately account for frictional losses within the control volumes themselves—MELCOR does not calculate any loss terms based on volume-centered velocities (see Section 6.5).

The flow resistances (and open fractions) for specified flow paths involving core cells are automatically adjusted to represent partial or total blockage of the flow by core debris, as calculated by the COR package. See Section 6.7 for a discussion of this model.

5.4.1 Flow Path Segments

If a flow path *j* is imagined to consist of a number of pipe-like segments, the total frictional pressure drop for phase φ (*P* or *A*) is given by

$$\Delta P^{f}_{j,\varphi} = \frac{1}{2} K_{j,\varphi} \rho_{j,\varphi} \left| v_{j,\varphi} \right| v_{j,\varphi} + \sum_{s} \frac{2 f_{\varphi,s} L_s}{D_s} \rho_{\varphi,s} \left| v_{\varphi,s} \right| v_{\varphi,s} \qquad (5.42)$$

where K is the form loss coefficient for the entire flow path, and f is the Fanning friction coefficient for segment s, which has length L_s and hydraulic diameter D_s. The sum is over the segments in the flow path.

In Equation (5.42), the pressure drops associated with sudden area changes or bends (the K term) and wall friction losses for the pipe segments (the f terms) are quadratic in velocity but, as written, each term involves a different velocity. For each flow path, MELCOR computes phase velocities $v_{j,P}$ and $v_{j,A}$ for the pool and the atmosphere. These define the volumetric flow of pool and atmosphere through the flow path,

$$J_{j,\varphi} = \alpha_{j,\varphi} F_j A_j v_{j,\varphi} \tag{5.43}$$

where A_j is the flow path area and F_j is the fraction of that area which is open. If the flow is assumed to be incompressible, i.e., $\rho_{\varphi,s} = \rho_{j,\varphi}$, the volumetric flow of each phase in the segments is constant, and the segment velocities are given by

$$v_{\varphi,s} A_s = v_{j,\varphi} F_j A_j \tag{5.44}$$

where A_s is the segment area. (Note that if a segment is to represent a number of parallel pipes, A_s should be the total flow area while D_s should be the hydraulic diameter of each pipe.) Therefore, all the loss terms may be combined to give an effective loss coefficient K.

$$K^*_{j,\varphi} = K_{j,\varphi} + \sum_s \frac{4 f_{\varphi,s} L_s}{D_s} \left(\frac{F_j A_j}{A_s} \right)^2 \tag{5.45}$$

The frictional pressure loss can be cast in the following form

$$\Delta P^f_{j,\varphi} = \frac{1}{2} K^*_{j,\varphi} \rho_{j,\varphi} \left| v_{j,\varphi} \right| v_{j,\varphi} \tag{5.46}$$

The input form-loss coefficient for positive or negative flow (FRICFO or FRICRO on input record FLnnn03) is used for $K_{j,\varphi}$ depending on the sign of $v_{j,\varphi}$.

The wall-friction terms are calculated following the method of Beattie and Whalley [15]. A mixture Reynolds number is defined for each segment as

$$\mathrm{Re}_s = \frac{\left(\alpha\,\rho_A|v_A| + (1-\alpha)\rho_P|v_P|D_s\right)}{\mu_m}\left(\frac{F_j A_j}{A_s}\right) \tag{5.47}$$

using a mixture viscosity

$$\mu_m = \alpha\,\mu_A + (1-\alpha)(1+2.5\alpha)\mu_P \tag{5.48}$$

Here μ_A is calculated by the MP Package for a mixture of gases with the composition of the atmosphere. The viscosity of liquid water is used for μ_P (despite the fact that the pool may contain bubbles). Note that μ_m has the proper limits (μ_P or μ_A, respectively) as α goes to 0.0 or 1.0.

The flow-path void fraction computed by MELCOR (Section 5.2.1) is used in Equations (5.47) and (5.48) rather than the homogeneous void fraction originally proposed in Reference [15]. The constants in Equation (5.48) are coded as sensitivity coefficients in array C4404, and may therefore be modified by user input if desired.

The Reynolds number calculated from Equation (5.47) is used in a standard single-phase-flow friction correlation (which will be described in Section 5.4.2) to determine a single-phase friction factor f_1, which is used directly for f_P.

The flow quality,

$$x = \frac{\alpha\,\rho_A v_A}{\alpha\rho_A v_A + (1-\alpha)\rho_P v_P} \tag{5.49}$$

is used to interpolate the atmosphere friction factor f_A linearly between the single-phase value f_1 when only atmosphere is flowing in the path (x = 1.0) and zero for $x \le x_0$. [x_0 is coded as sensitivity parameter (C4404(12), with a default value of 0.9.) This is intended to reflect the tendency toward annular flow, with the gas phase preferentially occupying the center of a flow path, away from the walls and therefore not directly affected by wall friction.

The wall friction terms depend only on the velocity in the segment. Therefore, for a given volumetric flow (Equation (5.43)), they are independent of F (the fraction of the flow path which is open). This is as it should be, since F is intended to model a local restriction such as a valve which has no effect on wall losses in pipe segments.

On the other hand, the entire form loss term (K) depends on the nominal flow path velocity which, for a given volumetric flow, is dependent on F. Thus, if F can vary (i.e., if the flow path contains a valve), F cannot be used to represent the effects of bends, contractions,

and/or expansions in that flow path. This is not a serious defect because such losses may be modeled using equivalent lengths of pipe [16] in the segment data; in addition, most valves are either fully open or closed, and the current form is correct in either case. At some later date, the restriction may be removed by allowing form loss coefficients to be input for each segment, in addition to this single coefficient now permitted for the path, with the segment form losses based on the segment velocities rather than the MELCOR flow path velocities.

5.4.2 Single-Phase Friction Factor

The single-phase friction factor correlation used in MELCOR includes laminar, turbulent, and transition regions. In the laminar region, $0 \le \mathrm{Re} \le 2000.0$, the expression used is

$$f = \frac{16.0}{\mathrm{Re}} \tag{5.50}$$

The Colebrook-White equation [17]

$$\frac{1}{\sqrt{f}} = 3.48 - 4.0 \log_{10}\left[\frac{2.0\,e}{D} + \frac{9.35}{\mathrm{Re}\sqrt{f}}\right] \tag{5.51}$$

is used in the turbulent region $\mathrm{Re} \ge 5000.0$. Here e is the surface roughness. This equation must be solved iteratively. In the transition region $2000.0 \le \mathrm{Re} \le 5000.0$, $\log(f)$ is linearly interpolated as a function of $\log(\mathrm{Re})$ between the limiting values for the laminar and turbulent regimes.

The various constants in these equations, including the limiting Reynolds numbers, are coded as sensitivity coefficients in the array C4404, and may therefore be modified by user input.

5.5 Interphase Forces

The force (momentum exchange) between pool and atmosphere flows sharing a single flow path is important both in entraining concurrent flows and in limiting countercurrent ones. In the latter case, it is responsible for the phenomenon of flooding, or countercurrent flow limitation (CCFL).

A model is required for use in MELCOR, but without the complicated flow-regime maps and constitutive equations of the type employed in TRAC [6] or RELAP5 [7]. Therefore, a simple form is used which will reproduce a flooding curve in the form given by Wallis [13]:

$$\left(j_g^*\right)^{\frac{1}{2}} + \left(j_f^*\right)^{\frac{1}{2}} = 1 \tag{5.52}$$

where $j_g \equiv \alpha v_g / v_1$ and $j_f \equiv (1-\alpha) v_f / v_0$ are scaled (dimensionless) volumetric flows of gas and fluid, respectively. In the following, we will adopt conventional MELCOR notation, where the conventional subscripts "*g*" and "*f*" become "A" and "P", respectively. As is shown in Appendix B, such a flooding curve will result if the relative velocity is modeled as a function of void fraction defined by

$$\frac{1}{v_r} \equiv \frac{1}{v_A - v_P} = \frac{\alpha}{v_1} + \frac{1-\alpha}{v_0} \tag{5.53}$$

Here v_1 and v_0 are the velocities used to scale j_A and j_P, respectively; they also turn out to be the limiting values of v_r for α, equal to 1.0 and 0.0, respectively.

Appendix B also shows that the steady (time-independent) solution of the two-phase momentum equation will agree with this result if the interphase force in Equation (4.6) is represented as

$$f_2 = g(\rho_P - \rho_A)\left(\frac{\alpha}{v_1} + \frac{1-\alpha}{v_0}\right) \tag{5.54}$$

In the interest of simplicity, only the form of v_0 and v_1 [18],

$$\frac{v_0}{v_1} = \sqrt{\frac{\rho_A}{\rho_P}} \tag{5.55}$$

is used in MELCOR to produce

$$f_2 = 900.\left[\alpha\sqrt{\rho_A} + (1-\alpha)\sqrt{\rho_P}\right] \tag{5.56}$$

in SI units. The constant chosen gives a value of about 0.3 m/s for the limiting relative velocity as α goes to zero for vertical flow of gas and normal density water, corresponding to the terminal rise velocity of bubbles. This equation is applied to all geometries, and the results are usually qualitatively acceptable. The term $f_{2,j}$ in the finite-difference Equation (4.23) is multiplied by the length over which the interphase force acts rather than the inertial length of the flow path. A distinct length is used for momentum exchange. The default is taken as the inertial length for horizontal flow paths and as the difference in

elevation between the lowest point and the highest point in the flow path (including junction openings) for vertical ones. Optional user input on record FLnnn05 is allowed to override these defaults for application to special geometries.

5.6 Pumps and Fans

A pump or fan model provides a functional relationship between the pressure head developed by such a device and the volumetric flow through it, with the operating speed as a parameter. Two models are currently available in MELCOR. One simply uses a control function to define the pressure head; this gives the user great flexibility, but requires that he accept complete responsibility for the results. An example of how this approach could be used to build a conventional homologous model for a reactor coolant pump is outlined in the Control Functions Users' Guide. The second model, referred to as "FANA," was originally intended to model a containment fan, but has also been used as an approximate representation of a constant-speed coolant pump in many calculations.

5.6.1 The FANA Model

This model was originally constructed to represent a simple fan, intended to move air (atmosphere) from compartment to compartment in containment. It can, however, be used to approximate a constant-speed coolant pump by appropriate choice of input parameters.

In the model, a parabolic relationship is assumed between the head, ΔP, developed by the fan and the volumetric flow, $\dot{V}$ through it. Three parameters define the resulting curve:

(1) the maximum pressure head developed, ΔP_M,

(2) the corresponding volumetric flow, $\dot{V}_M$, and

(3) the volumetric flow , $\dot{V}_0$, at which the head is zero.

For a given volumetric flow $\dot{V}$, the pressure head is then given by

$$\left(\frac{\Delta P}{\Delta P_M}\right)^2 = \begin{cases} 1 & \dot{V} < \dot{V}_M \\ \dfrac{\dot{V}_0 - \dot{V}}{\dot{V}_0 - \dot{V}_M} & \dot{V}_M \le \dot{V} \le \dot{V}_0 \\ 0 & \dot{V}_0 < \dot{V} \end{cases} \tag{5.57}$$

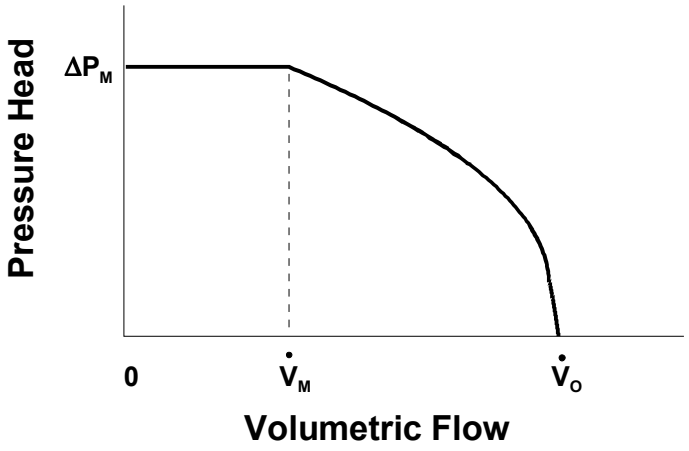

Figure 5.2 Fan Model Operating Characteristics

The resulting curve is illustrated in Figure 5.2. Suitable parameters may usually be chosen by comparison of this figure with the constant-speed operating curve for the device in question (in the normal operation quadrant).

The “forward” direction for a pump need not correspond to the direction of positive flow in the associated flow path. The necessary sign conventions for treating a reversed pump are described in the FL Package Users’ Guide.

A pump may be specified to be always on, or its operation may be controlled by a tabular function of time or by a control function of other arguments in the MELCOR database. The pump is off if the function is zero and on if it is non-zero. The model is implemented as an explicit momentum source, based on start-of-system-timestep velocities. Any functions which control the pump are also evaluated at the start of the MELCOR system timestep and treated as constant over the entire step.

6. Other Models

6.1 Bubble Physics

If a flow of atmospheric materials enters a control volume below the elevation of the surface of the pool in that volume, it must pass through the pool to reach its final destination. This process is visualized as involving rising bubbles in the pool, and the user may specify that an interaction be allowed based on a parametric model of thermal and condensation/evaporation physics. If this option is not selected, no interaction occurs and the transported atmospheric materials are simply added, unchanged, to the atmosphere in the acceptor volume. A separate pool scrubbing calculation may be done in the RN package using the SPARC90 model [19].

The physics modeled involves breakup of the injected gas stream into a swarm of bubbles, thermal equilibration of the gases with the pool, and saturation of the bubbles with water vapor at local conditions. These bubbles are not considered to reside in the pool, and do not contribute to pool swelling. The efficiency of the mass and energy transfer processes is affected by two factors, which are treated as independent.

The distance that gases must rise in order to reach the surface of the pool is involved in the breakup of the stream and the corresponding increase in surface area. It is modeled as an efficiency, ε_z, represented as

$$\varepsilon_z = \frac{z_P - z_J - 0.01\text{m}}{1.0\,\text{h}}, 0 \le \varepsilon_z \le 1 \tag{6.1}$$

where z_P is the elevation of the pool surface in the acceptor volume; z_J is the junction elevation in the acceptor volume; and h is the height of the junction opening.

That is, there is assumed to be no breakup until the bubbles have risen at least 1 cm, and breakup is assumed to be complete if they must rise through the junction opening height plus 1 cm.

The effect of subcooling of the pool is represented as the efficiency

$$\varepsilon_T = \frac{T_{sat}(P) - T_P - 0.1\text{K}}{5.0\,\text{K}}, 0 \le \varepsilon_T \le 1 \tag{6.2}$$

This requires subcooling by at least 0.1 K for any effect, and by at least 5.1 K for the maximum possible effect to be predicted.

The overall efficiency is taken as the product of these two efficiencies

$$\varepsilon = \varepsilon_z \varepsilon_T \tag{6.3}$$

If only water vapor and fog are present in the bubbles, it is assumed that a fraction ε of the vapor condenses, and an equal fraction of the fog in the flow path is deposited in the pool, with the remainder passing through to the atmosphere; no modification is made to the specific enthalpy (temperature) of material which passes through. In this case, the entire flow will be deposited in the pool if the depth and subcooling are adequate.

If noncondensible gases are present, and the depth and subcooling are sufficiently large, it is assumed that bubbles leave the pool at the pool temperature and, further, that the relative humidity in the bubbles will be 0.99, i.e., that the partial pressure of water vapor will

be 0.99 of the saturation pressure at the pool temperature. If $\varepsilon = 1$ as calculated from Equations (6.1), (6.2), and (6.3), this result is used directly, while the trivial result for no interaction is used for $\varepsilon = 0$. For $0 \le \varepsilon \le 1$, a linear interpolation (on the overall ε, Equation (6.3)) is performed between these limits. As in the case of no noncondensibles, a fraction ε of the fog flow is assumed to be deposited in the pool, with the remainder transmitted to the atmosphere.

All constants in this model (those in Equations (6.1) and (6.2)), and the limiting relative humidity) are coded as sensitivity coefficients, included in array C4405, and may therefore be modified by user input. The default values are those discussed here.

The effects of this model are implemented by appropriately modifying the definitions of donor properties; the normal donor properties are used for removal of atmospheric material from the actual donor volume, but a modified set of properties is used for the acceptor volume to which they are added. Specifically, if the volume of atmosphere moved through the flow path is

$$\left|\Delta V_j\right| = \alpha_j F_j A_j \left|\Delta V_{j,A}\right| \Delta t \tag{6.4}$$

the masses and energies removed from the donor volume, *d*, are

$$\Delta M_{m,d} = -\left|\Delta V_j\right| \frac{M_{m,d}}{V_{A,d}} \tag{6.5}$$

$$\Delta E_{A,d} = -\left|\Delta V_j\right| \frac{H_{A,d}}{V_{A,d}} \tag{6.6}$$

where, of course, the material index *m* in Equation (6.5) is limited to materials in the atmosphere. The masses added to the acceptor volume, *a*, however, have the more general form

$$\Delta M_{m,a} = \rho^*_{m,a} \left|\Delta V_j\right| \tag{6.7}$$

$$\Delta E_{A,a} = (\rho\, h)^*_{A,a} \left|\Delta V_j\right| \tag{6.8}$$

$$\Delta E_{P,a} = (\rho\, h)^*_{P,a} \left|\Delta V_j\right| \tag{6.9}$$

where *m* in Equation (6.7) includes the pool. The bubble physics model gives the masses and energies delivered to the acceptor volume ($\Delta M_{m,a}, \Delta E_{A,a}$ and $\Delta E_{P,a}$) in terms of the

entering masses and energies ($\Delta M_{m,d}$ and $\Delta E_{A,d}$). Therefore, Equations (6.7) through (6.9) serve as *definitions* of the quantities $\rho^*_{m,a}$, $(\rho\, h)^*_{A,a}$, and $(\rho\, h)^*_{P,a}$, which are subject to the constraints

$$\rho^*_{1,a} + \rho^*_{2,a} + \rho^*_{3,a} = \frac{M_{2,d} + M_{3,d}}{V_{A,d}} \tag{6.10}$$

$$\rho^*_{n,a} = \frac{M_{n,d}}{V_{A,d}} \qquad n \geq 4 \text{ (NCG)} \tag{6.11}$$

$$(\rho\, h)^*_{P,a} + (\rho\, h)^*_{A,a} = \frac{H_{A,d}}{V_{A,d}} \tag{6.12}$$

For atmospheric materials, the differences reflect the changes in composition and specific enthalpy described above; the pool terms reflect heat and mass exchange with the pool. If evaporation takes place, $\rho^*_{1,a}$ can be negative. In this case, it is further constrained so that use of Equation (6.7) does not result in a negative pool mass.

6.2 Time-Dependent (Specified) Flow Paths

The velocity in any flow path may be defined by the user, either as a Tabular Function of time or as a Control Function of other arguments in the MELCOR database. The resulting velocity is imposed on both pool and atmosphere (if present), with the void fraction computed using the standard model described in Section 5.2.

6.3 Critical Flow Models

After the solution of the flow (momentum) equation is complete, the computed flow in each flow path is compared with a calculated critical flow to determine if choking should be imposed. The test is bypassed if neither the pool velocity nor the atmosphere velocity is greater than a threshold of 20.0 m/s, coded as a sensitivity coefficient in C4402. If the flow exceeds the critical value, the flow path is added temporarily to a list of specified-flow flow paths, and the entire solution is repeated with the velocity constrained to be the critical value.

If only atmosphere is flowing through the path, the critical mass flux is taken as the sonic flux at the minimum section. For an ideal gas, this may be related to the sonic flux at stagnation conditions through the relation [20]

$$G_{C,A} = \rho_A^d C_{s,A}^d \left(\frac{2}{\gamma+1} \right)^{\left[\frac{\gamma+1}{2(\gamma-1)} \right]} \tag{6.13}$$

where $G \equiv \rho v$ is mass flux; subscript C denotes "critical"; C_s is the sonic velocity; and $\gamma \equiv c_p / c_v$ is the ratio of the specific heat at constant pressure to that at constant volume.

The use of the superscript "d" reflects the fact that in MELCOR the donor volume is assumed to be at stagnation conditions. The sonic velocity is evaluated in the CVT package. The multiplier is only a very weak function of γ, having a value within 5% of 0.58 for $1.1 \le \gamma \le 1.8$, and is therefore evaluated at a nominal value of $\gamma = 1.4$. There are two factors contributing to this function of γ:

(1) reduction in density because of expansion and

(2) reduction in sound speed because of cooling between stagnation conditions and the minimum section.

CONTAIN [3] includes both factors, HECTR [2] only the latter.

If only pool is flowing, the RETRAN [21] model (to be discussed in Section 6.3.1) for the critical mass flux is used, based on the pressure and specific enthalpy of the pool,

$$G_{C,P} = G_{C,RETRAN}\left(P^d, h_P^d\right) \tag{6.14}$$

If both phases are flowing, the critical mass flux is taken as a weighted average of that for the two phases,

$$\frac{\alpha\, \rho_A^d + (1-\alpha)\rho_P^d}{G_{C,2ph}} = \frac{\alpha\, \rho_A^d}{G_{C,A}} + \frac{(1-\alpha)\rho_P^d}{G_{C,P}} \tag{6.15}$$

This rather peculiar averaging scheme was motivated by the observation that it provides an almost exact representation of the Moody choking model if $G_{C,P}$ and $G_{C,A}$ are replaced by $G_{C,Moody}\ (\alpha = 0)$ and $G_{C,Moody}\ (\alpha = 1)$, respectively (see Appendix C).

If the mass flux evaluated using the new velocities calculated by the momentum equation exceeds the appropriate critical value, the velocity imposed (on both phases) is

$$v_{C,J} = \frac{G_C}{\alpha_J \rho_A^d + (1-\alpha_J)\rho_P^d} \tag{6.16}$$

Possible improvements in this model are described in Section 7.2.

Discharge coefficients are available (on FLnnn03 input records) as multipliers for the critical flow values calculated by these models. Different values may be used for forward (positive) and reverse (negative) flows in each flow path; the default values are 1. The appropriate discharge coefficient is included both in the test for choking in each flow path and in the velocity imposed if choking is detected. Use of a very large value is the only way to eliminate the possibility of choking in a flow path.

6.3.1 RETRAN Critical Flow Model

The RETRAN critical flow model consists of two 36-parameter, double-polynomial fits to extended Henry-Fauske critical flow for subcooled water (below and above 300 psia), and two 36-parameter fits to Moody critical flow for saturated (two-phase) water (below and above 200 psia), all as functions of stagnation pressure and enthalpy. It also includes a 9-parameter expression for a "transition" enthalpy as a function of pressure. A linear transition is constructed between the Henry-Fauske model at and below this enthalpy and the Moody model at and above saturation. The reader is referred to Reference [21] for a description of the basic models and the fitting procedure employed.

Two modifications to the RETRAN model were made for use in MELCOR. First, the fits are stated in Reference [21] to be valid only above 170 Btu/lbm, and were observed to yield unreasonable (sometimes negative) values not far below this value. Therefore, a linear interpolation was introduced between the fit at the lower limit of its applicability and the solution for orifice flow.

$$G_O = \sqrt{2P\,\rho_P} \tag{6.17}$$

imposed at $h_P = 0$. Second, it was observed that the transition enthalpy, which defined the upper bound for application of the Henry-Fauske model, was calculated as greater than the enthalpy of saturated liquid at the lower end of the pressure range (below about 21 psia). Therefore, the transition enthalpy was further bounded to be at least 10 Btu/lbm below saturation.

The fits themselves leave something to be desired; they appear to be excessively complicated, include modest discontinuities (several percent) at region boundaries, and have terrible extrapolation properties. Plans for improvement are described in Section 7.2.

6.4 Valves

A valve may be included in any flow path in MELCOR. Its operation is modeled as a change in the fraction of the area of the flow path which is open. This fraction may be defined directly as a Tabular Function of time, or as a Control Function of other arguments in the MELCOR database. Trips may also be used to model irreversible changes in flow areas such as ruptures of vessels or compartment walls, or to model the hysteresis in the operation of, say, a relief valve. The open fraction is limited to the range $0.0 \le F \le 1.0$ and, if the controlling function returns a value outside this range, it will be suitably truncated. The upper bound corresponds to a flow area equal to that input for the flow path, the lower bound to a closed path in which no flow is permitted.

Flow paths can be defined to permit only one-way flow, either forward or reverse. Such flow paths provide a simple way to represent idealized check valves. MELCOR also allows the open fractions (and flow resistances) for specified flow paths involving core cells to be automatically adjusted to represent partial or total blockage of the flow by core debris, as calculated by the COR package. See Section 6.7 for a discussion of this model.

6.5 Volume-Averaged Velocities

Volume-averaged (centered) velocities are used in MELCOR only in the calculation of forced-flow heat transfer coefficients (in a number of packages). This is because both control volume kinetic energies and momentum flux terms are neglected in the governing hydrodynamic equations. The only forced-flow heat transfer coefficients used in the CVH or FL packages are those associated with the pool atmosphere interface in nonequilibrium volumes (Section 5.1.2).

MELCOR is a lumped-parameter code which is often used to model three-dimensional volumes. A rigorously defined volume-averaged velocity would involve multi-dimensional effects, but the essential geometric information is simply not available. The model used in RELAP5 [7], which is also a lumped-parameter code, was considered for use in MELCOR. It may be written in the form

$$J_{V,\varphi} = \alpha_{V,\varphi} v_{V,\varphi} A_V = \frac{1}{2}\left(\sum_{j\ to\ V} J_{j,\varphi} + \sum_{j\ fm\ V} J_{j,\varphi} \right) \qquad \text{(RELAP5)} \qquad (6.18)$$

$$J_{j,\varphi} = \alpha_{j,\varphi} v_{j,\varphi} F_j A_j \qquad (6.19)$$

where J is volumetric flow; $\varphi = P\ or\ A$, and denotes pool or atmosphere; A_V is the flow area associated with volume V; α_V, φ are the area fractions for the volume flows; and all other symbols have been defined before. The sums in Equation (6.18) are over flow paths which connect *to* or *from* volume V.

Volume flows and velocities calculated from Equation (6.18) are strongly dependent on the logical direction of flow paths. For example, reversing both the sign of a velocity and the associated direction of positive flow (so that the actual volume moved from and the volume moved to are unchanged) does *not* preserve the volume flow. In particular, the net flow in a volume with a flow +*J to* it and +*J from* it is +J, while the net flow in a volume with +*J to* it and -*J to* it is zero. This is because it is assumed in the RELAP5 formulation that all *to* connections are on the left of a volume and all *from* connections on the right; in the second case cited above, the flows cancel and there is no resulting flow at the volume center.

We have found that this is often not the desired result in MELCOR nodalizations. Furthermore, the expected results cannot be obtained in any nodalization which connects volumes in a regular grid to approximate a finite-difference representation of a two-dimensional region; the best that can be done is to calculate the velocity *component* along one diagonal of the grid. Therefore, MELCOR uses a simplification of Equation (6.18) which treats all flow paths on an equal footing:

$$J_{v,\varphi} = \alpha_{V,\varphi} V_{v,\varphi} A_V = \frac{1}{2} \sum_j \left| J_{j,\varphi} \right| \qquad \text{(MELCOR)} \qquad (6.20)$$

where the sum is over all connected flow paths, and the void fraction associated with the volume flow is taken as a simple weighted average over connected flow paths in the form

$$\alpha_V = \frac{\sum_j \alpha_j F_j A_j}{\sum_j F_j A_j} \qquad (6.21)$$

This model can be understood qualitatively using the simple argument that, under steady conditions, a flow *through* a volume is counted twice: once where it enters the volume and once where it leaves. It makes no attempt to assign a direction to the volume velocity, and would therefore be unacceptable if it were necessary to calculate the momentum flux terms arising from $\nabla \cdot (\rho v v)$. In accord with this simple double-counting argument, a term is added to the sum in Equation (6.20) for the vapor flow to account for vapor generation in boiling in a nonequilibrium volume.

6.6 Special (Time-Specified) Volumes

MELCOR hydrodynamics allows boundary conditions to be defined by specifying the state of one or more volumes as functions of time. This is frequently necessary for simulation

of experiments. It is also useful for defining the outside-containment environment for a full reactor plant calculation.

In the simplest case, a volume may be specified as time-independent, with properties that do not change as the calculation progresses. Volumes can also be defined whose properties are maintained constant for a specified period of time, after which they are "freed" to function as normal volumes. This can simplify initialization of an operating steady state in a reactor. An initially time-independent pressurizer will enforce a constant pressure boundary condition, while initially time-independent steam generators enforce a constant thermal boundary condition during a pre-transient phase of the calculation.

In addition, several options are available for specifying the pressures, temperatures, and compositions of boundary volumes as functions of time, in terms of user-defined tabular functions, external data files, or control functions, as explained in the CVH Users' Guide.

A time-specified volume can serve any of the functions of a normal volume. It can provide boundary conditions for in- or out-flows, or for heat transfer. However, no volume-averaged velocity (Section 6.5) is calculated for a time-specified volume; forced convection heat transfer will therefore not be considered in the Heat Structure (HS) package. All phenomena modeled by the RadioNuclide (RN) package will be treated, with the sole exception that radionuclides are not allowed to advect *out* of such a volume. (This is intended to prevent radionuclides from reentering a failed containment building from the environment.) A time-specified volume can also be used in conjunction with a time-specified flow path (Section 6.2) to define a mass source with well-defined properties. This approach is particularly useful for water sources, for which temperature alone is insufficient to define the complete thermodynamic state; it also provides a way for gas sources to be made to participate in the bubble interactions described in Section 6.1.

Any mass or energy transferred to or from a time-specified volume is recorded as "created" in the CVH package for accounting purposes.

6.7 Core Flow Blockage

MELCOR includes a core flow blockage model to account for the changes in flow resistance in the degraded core states that will arise during a postulated reactor accident. It treats the entire range of degradation, from partially blocked rod geometry to debris bed geometry. The markedly increased resistance to flow in severely degraded geometries is particularly important because it will limit the flow available both to carry away decay heat and to provide steam for core oxidation. In addition to improving the basic modeling, inclusion of blockage effects has been found to improve code performance, particularly when a detailed CVH nodalization is used in the core region. The neglect of blockage can lead to prediction of unphysically large flows through regions containing very little fluid; the material Courant condition will then force extremely small timesteps, greatly increasing execution times.

At the start of a MELCOR calculation the core will (usually) be in a state for which the representation of friction (in terms of user input for intact geometry) is appropriate. This will change, however, following relocation of core materials. The blockage model, when invoked, will modify flow areas and flow resistances to account for the effects of refreezing of conglomerate debris onto fuel rods and/or other structures, or a loss of simple rod geometry through the creation or relocation of particulate debris.

The current model considers two flow regimes. For severely damaged core geometries, after particulate debris has been formed, it uses correlations developed for flow in porous media. Until this occurs, a simple modification to the flow resistance in intact geometry is used to account for changes in flow area associated with refrozen conglomerate debris. (Clad ballooning, which would have a similar effect, is not modeled.) As currently coded, the switch in regimes is made on a flow path by flow path basis, triggered by the first appearance of particulate debris in any core cell associated with the flow path. When the uncertainty in predicting the actual geometry of core debris is considered, we believe that this simple treatment is adequate for MELCOR use.

6.7.1 Debris Geometry

There are several correlations for the pressure drop for flow in porous media that can all be represented in the general form

$$(\Delta P)_{pourous\ bed} = \frac{1}{2}\rho\, j^2 \frac{L}{D_p}\left(\frac{1-\varepsilon}{\varepsilon^3}\right)\left[C_1 + C_2\left(\frac{1-\varepsilon}{\mathrm{Re}}\right) + C_3\left(\frac{1-\varepsilon}{\mathrm{Re}}\right)^{C_4}\right] \qquad (6.22)$$

where j is the superficial velocity (volumetric flux), ε is the porosity of the medium, D_p is the effective particle diameter, and Re is the Reynolds number based on these quantities,

$$\mathrm{Re} = \frac{\rho\, j\, D_p}{\mu} \qquad (6.23)$$

The average velocity of fluid in the medium (strictly, the average of the *component* of that velocity that lies in the direction of positive net flow) is given by

$$v \equiv \frac{j}{\varepsilon} \qquad (6.24)$$

This is further discussed by Dobranich [22], who lists coefficients for four published correlations in a table equivalent to the one below.

Table 6.1 Coefficients in Friction Correlations for Porous Media

Correlation	C_1	C_2	C_3	C_4	Reference
Ergun (original)	3.5	300.	0.0	-	[25]
Modified Ergun (smooth)	3.6	360.	0.0	-	[23]
Modified Ergun (rough)	8.0	360.	0.0	-	[24]
Achenbach	1.75	320.	20.	0.4	[24]

This correlational form is used to calculate the effects of core blockage on flow resistance once particulate debris has been formed. The coefficients in the correlation were coded as a sensitivity coefficient array, with $C_i = C4413(i)$; default values for I = 1, 2, and 3 are those for the original Ergun Equation [25].

In any flow path for which the blockage model has been invoked, the average porosity, ε, of core cells in the flow path is calculated from the ratio of hydrodynamic volume to total volume in the cells. This accounts for the effects of particulate and refrozen ("conglomerate") debris as described in the COR Package Reference Manual. In addition, the open fraction, $F_j(t)$, for that flow path is set equal to the porosity, ε, as an internally defined valve model. As a result, the nominal velocity in the flow path, v_j, calculated by MELCOR is consistent with the velocity in Equation (6.24), so long as the nominal area of the flow path, A_j, is equal to the geometric area, A_{geo}, of the cell(s) involved. After particulate debris has been formed, the pressure drop, Equation (6.22), can be cast in the form of an effective loss coefficient as

$$K^* = K_{empty} + \left[C_1 + C_2 \frac{1-\varepsilon}{\mathrm{Re}} + C_3 \left(\frac{1-\varepsilon}{\mathrm{Re}} \right)^{C_4} \right] \frac{(1-\varepsilon)L}{\varepsilon D_p} \qquad (6.25)$$

to replace the "normal" value in Equation (5.46). Here, the Reynolds number expressed in terms of that nominal velocity is

$$\mathrm{Re} = \frac{\rho \varepsilon v_j D_p}{\mu} \qquad (6.26)$$

and a term K_{empty} has been added to define the flow resistance in the "empty" path that will result when no core materials remain, the porosity is 1.0, and the porous medium model—used outside its range of applicability—would predict no friction.

6.7.2 Interpretation of Flow Areas

The nominal area and the open fraction are specified as part of user input to the FL package. In the regular nodalization of a finite difference code, there would be no need to distinguish the nominal area associated with a cell-boundary flow from the geometric area of the associated cell boundary. However, the distinction is essential in a control volume code such as MELCOR, where the definition of control volume geometry is limited and arbitrary interconnection of volumes is allowed. This is because a flow path must be able to represent the connection of a duct or pipe to a room or plenum as well as the boundary surface between two sections of a larger room or volume.

To avoid complications, MELCOR requires that the nominal flow path area be equal to the geometric area of the core cell(s) for all flow paths in which the blockage model is used. In order to eliminate the need for changes to existing decks when flow blockage modeling is added, the user input area is replaced by the geometric area, and the initial open fraction is simultaneously redefined as the porosity associated with core cell(s) in the flow path, for all flow paths in which the blockage model is invoked. The redefined values are flagged in MELGEN and MELCOR output as having been modified by the Flow Blockage model.

This may modify the open area, F A, associated with the initial geometry, which will result in different values being calculated for the velocity. However, because the advection terms in MELCOR hydrodynamics depend only on the total volumetric flow

$$J_j = j_j A_j(t) = F_j(t) v_j(t) A_j \tag{6.27}$$

(see Equations (4.2) and (4.5)), as do the wall friction terms (see the discussion following Equation (5.42)), only the form loss coefficient used for intact geometry must be adjusted to compensate for the change in open area. (For more discussion, see the final report on the model in Reference [26].)

The input form loss coefficient is replaced by an “equivalent” coefficient, K_{eqv}, that is related to that input by the user through

$$\frac{K_{eqv}}{[F(0)A_{nom}]^2} = \frac{K_{input}}{(F_{input}A_{input})^2} \tag{6.28}$$

for which the calculated pressure drop in intact geometry will match that which would be calculated from the user-input area, open fraction, and form loss. All such values are flagged in MELGEN and MELCOR output as having been modified by the Flow Blockage model.

6.7.3 Transition between Intact and Debris Geometries

If there is a period before the first appearance of particulate debris in any core cell associated with a flow path during which there is conglomerate debris frozen onto fuel rods (or other structures), the resulting reduction in flow area is accounted for by modification of the calculation for intact geometry. The presence of such material will change the porosity and therefore the open fraction for a flow path. However, the contribution of wall losses, represented by segment data, ordinarily dominates the pressure drop and—as calculated—this contribution is independent of the open fraction of the flow path. Therefore, a multiplier is applied to the friction calculated for intact geometry to account for the actual change in flow area, fluid velocity, and wall friction resulting from the presence of conglomerate debris prior to rod failure. The modified pressure drop is calculated as

$$(\Delta P)_{net,transition} = \left[\frac{\varepsilon(0)}{\varepsilon(t)}\right]^2 (\Delta P)_{\text{int}act} \qquad (6.29)$$

7. Discussion and Development Plans

7.1 Interphase Forces

An assessment of the simple model for interphase forces (described in Section 5.5) appears to have eliminated the more obvious limitations of the previous implementation. Calculations need to be done and compared with data (as represented by more general slip correlations) to assess the overall adequacy of the revised model.

7.2 Critical Flow Modeling

Atmosphere velocities which are significantly supersonic have been observed in some calculations, despite the presence of the critical flow model. This can arise if the phase velocities calculated by the momentum equation are very different. (Because of its greater inertia, the velocity of the pool is sometimes much less than that of the atmosphere before choking is considered.) The problem is that the net mass flux, calculated with the disparate velocities, may be subcritical (according to the current calculational model) even though one velocity is supersonic.

The entire concept of choking in a two-velocity model may need further examination. In the short term, however, the introduction of the interfacial momentum-exchange term, by reducing the differences between the calculated phase velocities, has gone a long way toward eliminating this problem.

The relatively complicated fits [21] used for Moody and Henry critical flow are not particularly good (a few percent). They are each constructed for two pressure ranges, and exhibit discontinuities of several percent at the matching line. The extrapolation properties are poor; the extrapolation often goes negative just outside the fit region. We have found (see Appendix C) that there are simpler representations, with comparable or better accuracy and good extrapolation properties; we will implement them in MELCOR when time permits.

APPENDIX A: Sensitivity Coefficients

A number of sensitivity coefficients are available in the hydrodynamics (CVH and FL) packages. Their use is described in the Control Volume Hydrodynamics (CVH) Package Users' Guide, and most are mentioned at appropriate places in this Reference Manual. This appendix is intended to aid the user in finding those places.

Coefficient	Default Value	Units	Usage, Reference
C4400			**Timestep Control**
(1)	0.5	--	Equation (4.47)
(2)	0.9	--	Equation (4.48)
(3)	0.15	--	Not discussed in this manual. Used only if no flow paths.
(4)	0.05	--	Equation (4.45)
(5)	0.0	Pa	Equation (4.45)
(6)	0.1	--	Executive fallback, Section 4.3 and second paragraph after Equation (4.44)
(7)	0.0	Pa	Executive fallback, Section 4.3 and second paragraph after Equation (4.44)
(8)	0.1	--	Equation (4.46)
(9)	1.0	K	Equation (4.46)
(10)	0.2	--	Executive fallback, Section 4.3 and second paragraph after Equation (4.44)
(11)	1.0	K	Executive fallback, Section 4.3 and second paragraph after Equation (4.44)

Coefficient	Default Value	Units	Usage, Reference
C4401			**Velocity Convergence Criteria**
(1)	0.09	--	Section 4.3, following outline of strategy
(2)	0.0	m/s	Section 4.3, following outline of strategy,
(3)	0.0	--	Implies iteration limit. See discussion in Users' Guide.
(4)	0.0	--	Allows relaxed convergence tolerance. See Users' Guide.

Coefficient	Default Value	Units	Usage, Reference
C4402			**Minimum Velocity to be Considered for Choking**
(1)	20.0	m/s	First paragraph, Section 6.3

Coefficient	Default Value	Units	Usage, Reference
C4404			**Friction Factor Parameters**
(1)	3.48	--	Colebrook-White, Equation (5.51)
(2)	4.0	--	Colebrook-White, Equation (5.51)
(3)	2.0	--	Colebrook-White, Equation (5.51)
(4)	9.35	--	Colebrook-White, Equation (5.51)
(5)	1/ln(10)	--	Used in solution of Colebrook-White, should not be modified
(6)	1.0	--	Two-phase viscosity, Equation (5.48)
(7)	14.14	--	Used in solution of Colebrook-White, should not be modified
(8)	0.0005	--	Used in solution of Colebrook-White, should not be modified
(9)	0.0	--	Used in solution of Colebrook-White, should not be modified
(10)	1.0	--	Two-phase viscosity, Equation (5.48)
(11)	2.5	--	Two-phase viscosity, Equation (5.48)
(12)	0.9	--	Bound for atmosphere friction, text following Equation **Error! Reference source not found.**
(13)	16.0	--	Laminar friction, Equation (5.51)
(14)	2000.0	--	Limiting Reynolds Number, text following Equation (5.51)
(15)	5000.0	--	Limiting Reynolds Number, text following Equation (5.51)

Coefficient	Default Value	Units	Usage, Reference
C4405			**SPARC Bubble Physics Parameters**
(1)	0.01	m	Minimum rise distance, Equation (6.1)
(2)	1.0	--	Rise scale, Equation (6.1)
(3)	0.1	K	Minimum subcooling, Equation (6.2)
(4)	5.0	K	Subcooling scale, Equation (6.2)
(5)	0.99	--	Exit relative humidity, text following Equation (6.3)

Coefficient	Default Value	Units	Usage, Reference
C4406			**Maximum Allowed Fog Density**
(1)	0.1	kg/m^3	Text of Section 5.1.4

Coefficient	Default Value	Units	Usage, Reference
C4407			**Pool/Atmos Heat/Mass Transfer Parameters**
(1)	0.3	m/s	Bubble rise velocity, second paragraph, Section 5.1.3
(2)	0.02	--	Forced convection, Equation (5.21)
(3)	0.14	--	Turbulent free convection in atmosphere, Equation (5.23)
(4)	1/3	--	Turbulent free convection in atmosphere, Equation (5.23)
(5)	0.54	--	Laminar free convection in atmosphere, Equation (5.23)
(6)	1/4	--	Laminar free convection in atmosphere, Equation (5.23)
(7)	0.27	--	Turbulent free convection in pool, Equation (5.22)
(8)	1/4	--	Turbulent free convection in pool, Equation (5.22)
(9)	0.27	--	Laminar free convection in pool, Equation (5.22)
(10)	1/4	--	Laminar free convection in pool, Equation (5.22)
(11)	0.4	--	Maximum pool void, text following Equation (5.31)
(12)	0.9	--	Maximum condensation fraction, text following Equation (5.15)

Coefficient	Default Value	Units	Usage, Reference
C4408			**Pressure Iteration Parameters**
(1)	0.0	--	Decimal digits used to disable several models (for debugging)
(2)	0.005	--	Subcycle step increase, pressure convergence, Equation (4.44)

Coefficient	Usage, Reference
C4409	**Limits and Tolerances for Time-Specified Volumes**
(1-6)	These coefficients are used to test the acceptability and consistency of user input for time-specified volumes. They are not discussed in this reference manual; the description in the users' guide is complete and self-contained.

Coefficient	Default Value	Units	Usage, Reference
C4410			**Vapor Velocity Enhancement during Direct Containment Heating**
(1)	1.0	--	Multiplier on volume-averaged velocity
(2)	1500.0	K	Minimum temperature of airborne debris for application
			These coefficients can be used to increase heat transfer from the atmosphere of a volume in which direct containment heating is occurring by parametrically increasing the atmosphere velocity that will be used in heat transfer correlations.

Coefficient	Usage, Reference
C4411	**Limits and Tolerances for Iterations in the CVT Package**
(1-3)	These coefficients are used to control iterative calculations in the CVT package. They are not discussed in this reference manual; the description in the users' guide is complete and self-contained.

Coefficient	Default Value	Units	Usage, Reference
C4412			**Limits and Tolerances for Iterations in the CVH Package**
(1)	0.01	--	Void fraction convergence, discussion in Section 4.3

Coefficient	Default Value	Units	Usage, Reference
C4413		--	**Flow Blockage Friction Parameters**
(1)	3.5	--	Equations (6.22) and (6.25)
(2)	300.0	--	Equations (6.22) and (6.25)
(3)	0.0	--	Equations (6.22) and (6.25)
(4)	0.4	--	Equations (6.22) and (6.25)
(5)	1.0E-6	--	Minimum porosity to be used in Equations (6.22) and (6.25)

Coefficient	Default Value	Units	Usage, Reference
C4414			**Hydrodynamic Volume Fraction**
(1)	1.0E-4	--	Minimum fraction of the initial volume in a control volume that will always be available to hydrodynamic

Coefficient	Default Value	Units	Usage, Reference
C4414			**Hydrodynamic Volume Fraction**
			materials, regardless of relocation of virtual volume.

APPENDIX B: The Interphase Force and the Flooding Curve

The interphase force results from exchange of momentum ("drag") between the two fields, pool and atmosphere in MELCOR, when they share a flow path. Many codes such as TRAC [6] and RELAP5 [7] contain detailed models for this force. These models are typically based on specific microscopic pictures of the state of the fluid, and therefore must contain a number of submodels for different flow regimes. There are at least two practical difficulties in constructing and validating such a model:

(1) The force is not directly measurable; all observable quantities result from delicate balances among this force, wall forces, and gravitational forces. Inertial forces are sometimes involved.

(2) Discontinuities between the submodels, or even a lack of smoothness in the transitions between them, can result in numerical problems so severe as to prevent calculation of acceptable solutions in any but the simplest cases.

Much of the complexity can be avoided—at the expense of accuracy in some cases—by considering only a single momentum equation, defining an average (mixture) velocity for the two fields, and modeling the relative velocity between them as a constitutive relation. In this approach, referred to as the "drift flux" model, the relative velocity is a function of the local conditions, but *not* of their history. RELAP4 [1] is typical of codes employing the drift flux model.

The drift flux model is conventionally cast in terms of the volumetric fluxes defined by

$$j_g \equiv \alpha v_g = \alpha j + \alpha \varepsilon v_r \tag{B.1}$$

$$j_g \equiv \varepsilon v_\ell = \varepsilon j - \alpha \varepsilon v_r \tag{B.2}$$

where

$$\varepsilon \equiv 1 - \alpha \tag{B.3}$$

$$j \equiv j_g + j_\ell \tag{B.4}$$

$$v_r \equiv v_g - v_\ell \tag{B.5}$$

and the fields are identified as ℓ and *g*, denoting "liquid" and "gas." (Note that the natural dimensions of the volumetric fluxes, $m^3 / m^2 \bullet s$, are the same as those of the velocities.) In these relations, v_r or, more usually,

$$j_{g,j} \equiv \alpha \, \varepsilon \, v_r \tag{B.6}$$

is considered to be defined by a constitutive equation as a function of α, densities, and geometry.

For a given value of α, the locus of possible values of j_g and j_ℓ as functions of j form a straight line, referred to as a *drift flux line*, as shown in Figure B.1.

The upper left-hand quadrant of Figure B.1 represents a region of countercurrent flow where no quasi-steady solutions are possible. The boundary of this region, formed by the envelope of the drift-flux lines and shown as a dashed curve in the figure, is called the *flooding curve*, and defines the limit of (quasi-steady) countercurrent flow. The curve may be parameterized by α, and represents the locus of points where

$$\left(\frac{\partial j_g}{\partial \alpha}\right)_j = 0. \tag{B.7}$$

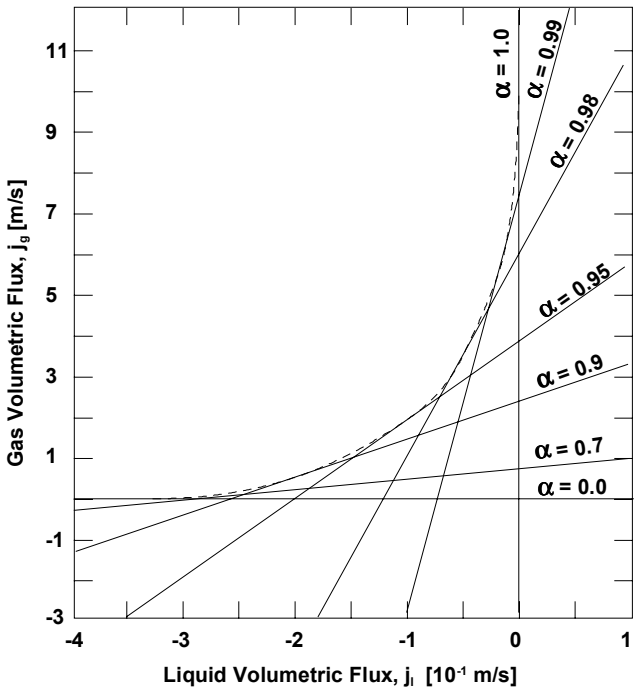

Figure B.1 Drift Flux Lines and the Flooding Curve

One empirical correlation which defines the flooding curve, as discussed by Wallis in Section 11.4 of Reference [13], has the form

$$\left(\frac{j_{g,F}}{v_1}\right)^{\frac{1}{2}} + \left(\frac{j_{\ell,F}}{v_0}\right)^{\frac{1}{2}} = 1. \tag{B.8}$$

Here $j_{g,F}$ and $j_{\ell,F}$ define a point on the flooding curve, and v_0 and v_1 are scaling velocities independent of α. Note that this equation is often written with a constant other than 1 on the right-hand side and/or with a coefficient multiplying either or both terms on the left-hand side; these can be absorbed into the scaling velocities without loss of generality.

It is a straightforward exercise to show that if

$$v_r(\alpha) = \frac{1}{\alpha/v_1 + \varepsilon/v_0} \tag{B.9}$$

the flooding curve defined by Equation B.7 is given by

$$j_{g,F} = \frac{\alpha^2/v_1}{(\alpha/v_1 + \varepsilon/v_0)^2}, \tag{B.10}$$

$$j_{\ell,F} = -\frac{\varepsilon^2/v_0}{(\alpha/v_1 + \varepsilon/v_0)^2} \tag{B.11}$$

Equations B.10 and B.11 clearly satisfy the Wallis flooding relation given by Equation B.8. In addition, they give a parameterization of that curve by the void fraction α. MELCOR uses velocities rather than volumetric fluxes as the basic variable. In terms of velocities, the parameterization is

$$\alpha_F = \frac{|v_{g,F}|/v_0}{|v_{g,F}|/v_0 + |v_{\ell,F}|/v_1} \tag{B.12}$$

The drift flux model is most often used for quasi-steady, nearly incompressible flow. It is relatively simple to ensure that a two-fluid model will give similar results in the corresponding regime. In this limit, where $\partial/\partial t \to 0$ and derivatives of density may be neglected, the momentum equations for the two fields—neglecting momentum flux $(v\partial v/\partial x)$ terms—may be written as

$$\alpha\frac{\partial P}{\partial x} = \alpha\,\rho_g g_x - \alpha\,F_g v_g - \alpha\,\varepsilon\,F_{\ell g}(v_g - v_\ell) \tag{B.13}$$

$$\varepsilon \frac{\partial P}{\partial x} = \varepsilon\, \rho_\ell g_x - \varepsilon\, F_\ell v_\ell - \alpha\, \varepsilon\, F_{\ell g}\left(v_\ell - v_g\right) \tag{B.14}$$

The coefficients F_g, F_ℓ, and $F_{\ell g}$ in the various momentum exchange terms are abbreviations for the usual $2 f\, \rho |v| / D$ terms, in the form most commonly employed in simulation codes for two-phase flow. In these equations, g_x is the component of the gravitational acceleration in the x direction; in particular, it is $-g$ if x is measured positive in the upward vertical direction.

If the pressure gradient is eliminated between Equations B.13 and B.14, the result can be cast in the form

$$j_g = \frac{\alpha\left(F_\ell + F_{\ell g}\right)}{\alpha\, F_\ell + \varepsilon\, F_g + F_{\ell g}}\, j - \frac{\alpha\, \varepsilon\, \left(\rho_\ell - \rho_g\right) g_x}{\alpha\, F_\ell + \varepsilon\, F_g + F_{\ell g}} \tag{B.15}$$

Comparison of this equation with Equation B.1 shows that the quasi-steady solutions of the two-fluid equations will have a relative velocity given by

$$v_r = -\frac{\left(\rho_\ell - \rho_g\right) g_x}{\alpha\, F_\ell + \varepsilon\, F_g + F_{\ell g}} \tag{B.16}$$

and comparison of this result with Equation B.9 suggests that the interphase force be defined by

$$\alpha\, F_\ell + \varepsilon\, F_g + F_{\ell g} = \left(\rho_\ell - \rho_g\right) g_x \left(\alpha / v_1 + \varepsilon / v_0\right) \tag{B.17}$$

In MELCOR, we are most concerned with the flooding curve, which defines the limit of countercurrent flow. In most cases of interest, the net wall force, $F_\ell + F_g$, is small compared to the interphase force when flooding occurs. Therefore, wall forces are neglected in Equation B.17, and the interphase force term, $F_{\ell g}$, is set directly equal to the right-hand side of this equation.

Finally, when the differential form of the momentum equation is integrated from volume center to volume center, the integral of $g_x dx$ becomes $-g\Delta z$.

APPENDIX C: Moody Critical Flow

During evaluation of critical flow models for incorporation into MELCOR, the Moody critical flow tables in RELAP4 [1] were compared with the analytic fits in RETRAN [21] for atmospheric and higher pressures. The two representations agree within a few percent in general, and within a few tenths of 1 percent at reactor operating pressures.

The data for each pressure were found to be fit extremely well by the simple expression

$$\frac{\rho_m}{G_c(\alpha)} = \frac{\alpha\,\rho_g}{G_c(1)} + \frac{(1-\alpha)\rho_\ell}{G_c(0)} \tag{C.1}$$

where

$$\rho_m \equiv \alpha\,\rho_g + (1-\alpha)\rho_\ell \tag{C.2}$$

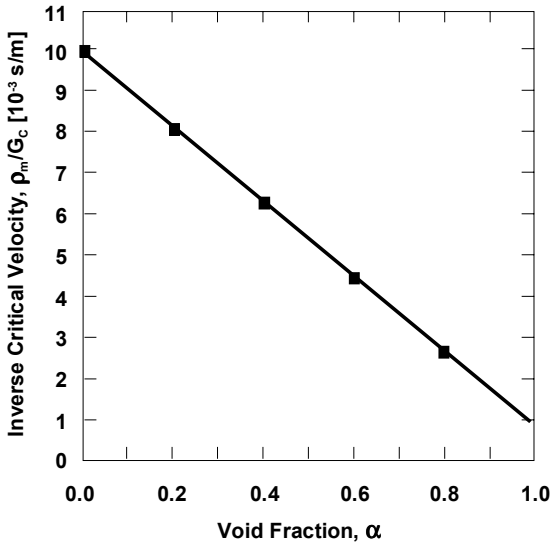

Figure C.1 Moody Critical Flow Data and Approximate Fit

is the mixture density. Equation C.1 states simply that the inverse of the mass-averaged velocity in critical flow is a linear function of the void fraction based on the critical flows at qualities of 1.0 and 0.0. We know of no theoretical basis for this, but the fit is quite good. Figure C.1 shows a typical example. The data are from the RETRAN fits for a pressure of 400 psia; the dashed line shows an approximate linear representation.

References

1. RELAP4/MOD5 A Computer Program for Transient Thermal-Hydraulic Analysis of Nuclear Reactors and Related Systems User's Manual, Volume 1, RELAP4/MOD5 Description, ANCR-NUREG-1335, Idaho Nuclear Engineering Laboratory, Idaho Falls, ID (September 1976).

2. S. E. Dingman, et al., HECTR Version 1.5 User's Manual, NUREG/CR-4507, SAND86-0101, Sandia National Laboratories, Albuquerque, NM (April 1986).

3. K. K. Murata, et al., "Code Manual for CONTAIN 2.0: A Computer Code for Nuclear Reactor Containment Analysis," NUREG/CR-6533, SAND97-1735, 1997.

4. "MAAP4, Modular Accident Analysis Program User's Manual," Volumes 1 and 2, EPRI (1994).

5. JANAF Thermochemical Tables, Dow Chemical Company, Thermal Research Laboratory, Midland, MI (1965).

6. TRAC-PF1, An Advanced Best-Estimate Computer Program for Pressurized Water Reactor Analysis, NUREG/CR-3567, LA-9944-MS, Los Alamos National Laboratory, Los Alamos, NM (February 1984).

7. V. H. Ransom, et al, RELAP5/MOD1 Code Manual Volume 1. System Model and Numerical Methods; Volume 2: *Users Guide and Input Requirements*, NUREG/CR-1826, EGG-2070, Idaho National Engineering Laboratory (March 1982).

8. L. N. Kmetyk, MELCOR 1.8.1 Assessment: FLECHT SEASET Natural Circulation Experiments, SAND91-2218, Sandia National Laboratories, Albuquerque, NM (December 1991).

9. J. G. Collier, Convective Boiling and Condensation, 2nd ed., McGraw-Hill, New York (1981), p. 326.

10. R. B. Bird, W. E. Stewart, and E. N. Lightfoot, Transport Phenomena, John Wiley & Sons, New York (1960), Equation 18.4-25.

11. See, for example, W. H. McAdams Heat Transmission, McGraw Hill, New York (1959). The correlation for the atmosphere is for an unstable temperature gradient; that for the pool is for a stable gradient and a finite surface.

12. R. K. Cole, Jr., Letter Report to Ron Foulds, USNRC, "CVH Pool/Atmosphere Condensation," under FIN A 1339 (August 1992).

13. G. B. Wallis, One-dimensional Two-phase Flow, McGraw-Hill Book Company, New York, NY (1969), Chapter 9.

14. F. Gelbard and J. H. Seinfeld, "Simulation of Multicomponent Aerosol Dynamics," J. Colloid and Interface Science, **78** (2) (December 1980).

15. D. R. H. Beattie and P. B. Whalley, "A Simple Two-Phase Frictional Pressure Drop Calculational Method," Int. J. Multiphase Flow, **8** (1) pp. 83-87 (1982).

16. "Flow of Fluids through Valves, Pipes, and Fittings," Technical Paper 410, Crane Co., Chicago, IL (1969).

17. R. D. Blevins, Applied Fluid Dynamics Handbook, Van Nostrand Reinhold, New York (1984); Section 6.3, with conversion of the Darcy-Weisbach form to the Fanning form used in MELCOR.

18. G. B. Wallis, One-dimensional Two-phase Flow, McGraw-Hill, New York (1969), Section 11.4.

19. P. C. Owczarski and K. W. Burk, SPARC-90: A Code for Calculating Fission Product Capture in Suppression Pools, NUREG/CR-5765, PNL-7723 (October 1991).

20. R. B. Bird, W. E. Stewart, and E. N. Lightfoot, Transport Phenomena, John Wiley & Sons, New York (1960), Equation 15.5-42, with identification of the sound speed as $(\gamma P / \rho)^{1/2}$.

21. RETRAN-02—A Program for Transient Thermal-Hydraulic Analysis of Complex Fluid Systems, Volumes 1-3, NP-1850-CCM, Electric Power Research Institute, Palo Alto, CA (May 1981).

22. D. Dobranich, SAFSIM Theory Manual—A Computer Program for the Engineering Simulation of Flow Systems. SAND92-0693, Sandia National Laboratories, Albuquerque, NM (1993).

23 I. F. Macdonald, M. S. El-Sayed, K. Mow, and F. A. L. Dullien, "Flow Through Porous Media – the Ergun Equation Revisited," in Ind. Eng. Chem. Fundam., Vol. 18, No. 3, pp. 199-208, 1979.

24 E. Achenbach, "Heat Transfer and Pressure Drop of Pebble Beds Up to High Reynolds Number," in Proceedings of Seventh International Heat Transfer Conference, Vol. 1, pp. 3-8, 1982.

25. S. Ergun, “Fluid Flow Through Packed Columns,” in Chem. Eng. Progress, Vol. 48, No. 2, p. 504 (1952) (as cited in Reference 11).

26 R. K. Cole, Jr., “Incorporation of a Core flow Blockage Model into MELCOR,” letter report to John Ridgely, USNRC, November 30, 1995.